JGH Journal of Gastroenterology and Hepatology

JGHF

doi:10.1111/j.1440-1746.2010.06470.x

MECHANISMS OF GASTROINTESTINAL, PANCREATIC AND LIVER DISEASES

Animal model for study of human hepatitis viruses

Kazuaki Chayama,*,† C Nelson Hayes,*,† Nobuhiko Hiraga,*,† Hiromi Abe,*,† Masataka Tsuge*,† and Michio Imamura*,†

*Department of Medicine and Molecular Science, Division of Frontier Medical Science, Programs for Biomedical Research, Graduate School of Biomedical Sciences, Hiroshima University, and †Liver Research Project Center, Hiroshima, Japan

Key words
hepatitis B virus, hepatitis C virus, uPA/scid mouse model.

Accepted for publication 26 July 2010.

Correspondence
Professor Kazuaki Chayama, Department of Medical and Molecular Science, Division of Frontier Medical Science, Programs for Biomedical Research, Graduate school of Biomedical Science, Hiroshima University, 1-2-3 Kasumi, Minami-ku, Hiroshima 734-8551, Japan. Email: chayama@hiroshima-u.ac.jp

Abstract

Human hepatitis B virus (HBV) and hepatitis C virus (HCV) infect only chimpanzees and humans. Analysis of both viruses has long been hampered by the absence of a small animal model. The recent development of human hepatocyte chimeric mice has enabled us to carry out studies on viral replication and cellular changes induced by replication of human hepatitis viruses. Various therapeutic agents have also been tested using this model. In the present review, we summarize published studies using chimeric mice and discuss the merits and shortcomings of this model.

Introduction

Hepatitis B virus (HBV) and hepatitis C virus (HCV) are pathogens that cause chronic infection in humans. There are 360 million and 170 million people infected worldwide with HBV or HCV, respectively.[1,2] Infected individuals develop acute hepatitis, chronic hepatitis and liver cirrhosis. The viruses are also important causative agents of hepatocellular carcinoma, especially in the Asia–Pacific region.[3] Study of the biology and development of therapies for each virus has long been hampered by the lack of a small animal model that supports hepatitis virus infection. This is probably as a result of the lack of receptor molecules necessary for viral infection in animal liver cells.

Transgenic mice that express over-length HBV-DNA export viral particles into the serum,[4] and such animals can be used to evaluate antiviral agents,[5–7] as well as HBV-targeted siRNA[8]. However, the virus life cycle is not established in this model, and it is inappropriate for studying drug-resistant HBV strains. Accordingly, researchers attempted to transplant human hepatocytes into mice. The development of the trimera mouse was one such attempt, in which human hepatocytes were transplanted under the kidney capsule of immune-deficient mice after lethal irradiation.[9,10] However, the number of hepatocytes that could survive on the kidney capsule was small, and normal liver architecture was not present. Although 85% of HBV-inoculated animals developed HBV viremia, the titer was less than 10^5 virus particles or IU/mL.[9] Similarly, 85% of HCV-inoculated animals also developed viremia,[10] but the level of the viremia only reached 10^5/mL. Thus, the advent of human hepatocyte transplanted uPA/scid mice has provided the first really useful model for acute and chronic infections of human hepatitis virus.

Human liver cell transplanted uPA/scid mice

Transgenic mice in which the urokinase gene is driven by the human albumin promoter/enhancer were developed and shown to have accelerated hepatocyte death and consequent chronic stimulation of hepatocyte growth.[11] Transplanted rat hepatocytes proliferated and repopulated injured livers in immunodeficient uPA mice, which were produced by mating uPA transgenic mice with scid mice.[12] Human hepatocytes were then transplanted into uPA/scid mice; these cells proliferated and replaced the apoptotic mice liver cells (Fig. 1).

Such human hepatocyte chimeric mice have been shown to be susceptible to both HBV[16] and HCV[17] infections. Repopulation levels by human hepatocytes have been estimated by measuring human albumin levels in mouse serum. Replication levels of both HBV[13] and HCV[17] were higher in mice in which the repopulation index was higher. A unique attempt to remove mouse residual liver cells with the herpes simplex virus type-1 thymidine kinase (HSVtk)/ganciclovir (GCV) system failed to result in a higher repopulation rate as a result of damage to the transplanted human hepatocyte caused by bystander effects.[18] Despite this, mice with livers that have been highly repopulated with human hepatocytes

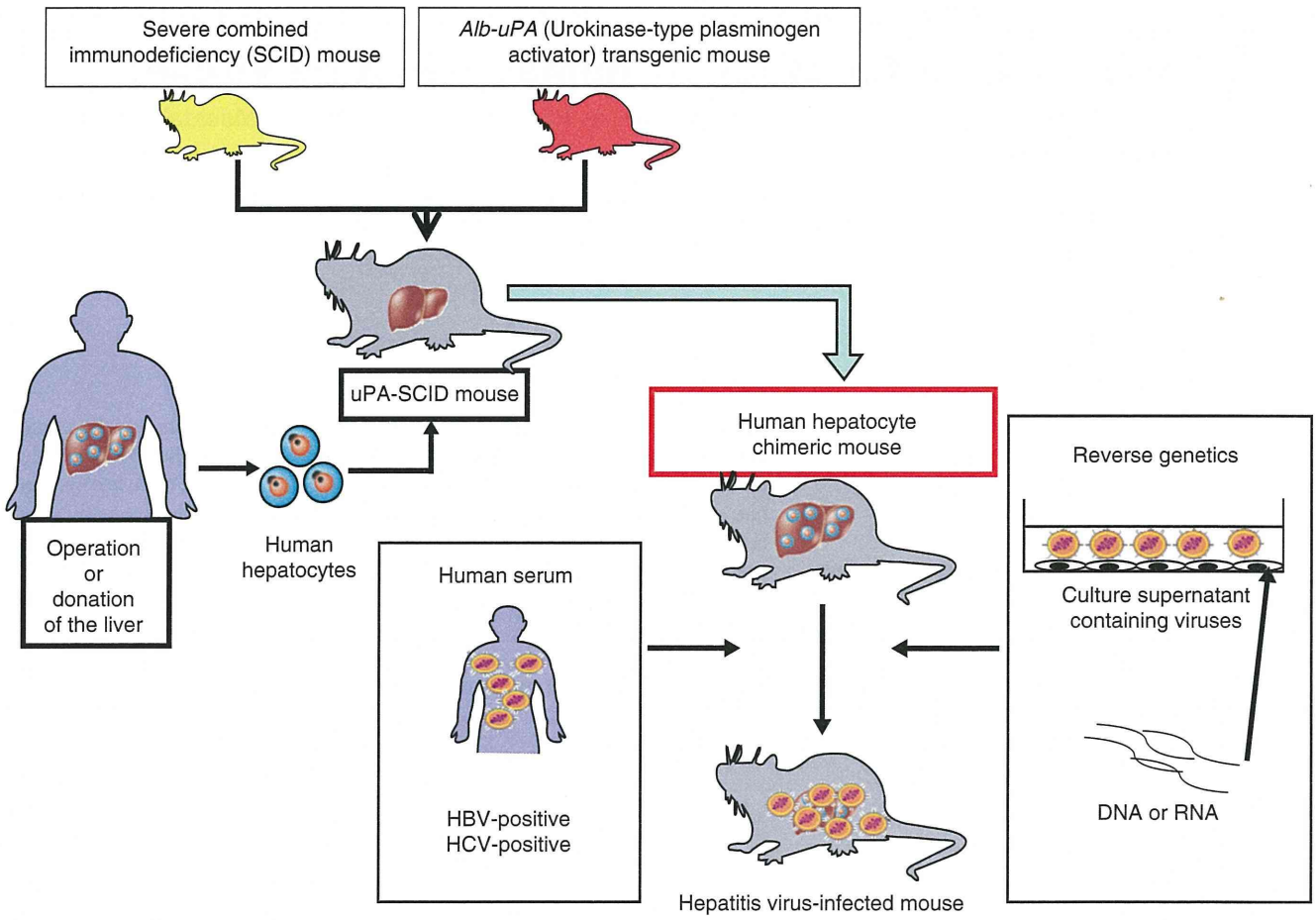

Figure 1 Generation of human hepatocyte chimeric mice and hepatitis virus infection model. A uPA/scid mouse was created by mating uPA transgenic mouse and scid mouse. Human hepatocytes obtained by surgical resection or donation were transplanted to newborn mice. The chimeric mice can be infected with hepatitis B virus (HBV) or hepatitis C (HBC) virus by injecting human serum containing these viruses. Alternatively, the mice can be infected by HBV[13] or HCV[14] created in cell culture or by injecting HCV RNA into the mouse liver.[15]

are susceptible to infection with both HBV and HCV, and as such comprised the most effective small animal model for chronic hepatitis so far developed.[19,20] An example of a highly repopulated mouse liver that we are using in experiments is shown in Figure 2.

Highly repopulated mice have been shown to be a valuable model for the study of drug metabolism.[21–29] Advances in technology for human hepatocyte transplantation have enabled serial passage of human hepatocytes in uPA/scid mice and have been shown to retain infectivity for HBV.[30]

This mouse model and other animal models for the study of hepatitis viruses have been summarized in reviews by Meuleman and Leroux-Roels,[31] Dandri *et al.*,[32,33] Barth *et al.*,[34] and Kneteman and Toso.[35] The present review will focus on key issues and updated information.

Study of hepatitis B virus infection using human hepatocyte chimeric mice

Since the initial reports of successful transmission of HBV to human hepatocyte chimeric mice in 2001 and 2004,[16,27] several researchers have reported transmission of HBV into similar mice.[13,36,37] In these studies, passage experiments studies show that HBV replicating in mice retain infectivity.[13,36] Further, the presence of viral proteins has been shown immunohistochemically in human hepatocytes transplanted into mouse livers, but these are not present in mouse hepatocytes.[13,36,37] Formation of viral particles in infected mouse livers can be shown by electron microscopy.[36,37] Genetically engineered viruses lacking HBe-antigen have also been shown to infect chimeric mice, proving that e antigen is dispensable for viral infection and replication.[13] In contrast, HBx protein has been shown to be indispensable for viral replication.[38] Transcomplementation of HBx protein with hydrodynamic injection restored HBV infectivity in mice. Interestingly, all revertant viruses show a restored ability to express HBx.[38]

By infecting chimeric mice with genotype A, B and C, differing proliferative capacity has been shown between HBV genotypes.[37] In mice infected for a relatively short time, there are no morphological changes in HBV infected mice livers in studies.[13,36] In contrast, the occurrence of liver cell damage has been reported after long-term infection of chimeric mice with HBV[39] or with specific strains of HBV;[40] these findings are consistent with direct cytopathic effects of HBV under certain conditions.

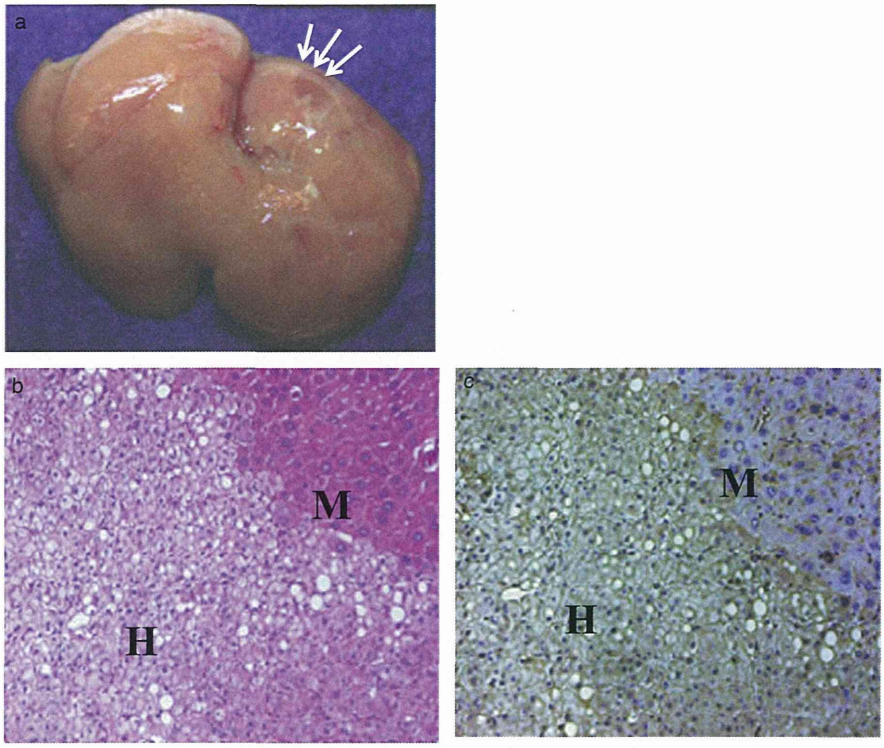

Figure 2 Representative uPA/scid mouse livers repopulated by human hepatocytes. (a) Mouse liver almost completely repopulated by human hepatocytes. Only a small portion of mouse hepatocytes are shown by arrows. (b) Microscopic figure of the mouse liver. M and H indicate regions consisting of mouse and human hepatocytes, respectively (Hematoxylin–eosin staining, magnification: ×100). (c) Microscopic figure of the mouse liver stained with antibody directed against human serum albumin.

The biological properties of a newly identified unique strain of HBV, genotype G, which replicates only in the presence of another genotype, were confirmed using the chimeric mouse.[41] Infectivity of another novel HBV strain, identified from a Japanese patient, that is divergent from known human and ape HBV has also been confirmed.[42] Titration of HBV infectivity, which previously could only be carried out using chimpanzees, can be carried out effectively using chimeric mice.[43]

Taking advantage of the absence of human immune cells in the chimeric mice, Noguchi *et al.*[44] showed that hypermutation of HBV increases in human hepatocytes under interferon treatment. Dandri *et al.* measured viral half-life in human and chimeric mice repopulated with wooly monkey hepatocytes.[45] The results clearly showed that viral half-life is shortened by immunological mechanisms in humans with low viral levels, but not in chimeric mice where functional immunity is absent. Hiraga *et al.*[46] showed an absence of interference between HBV and HCV.

Evaluation of therapeutic agents is the most important role for this mouse model. Tsuge *et al.*[13] assessed the effect of interferon and lamivudine using chimeric mice. Similarly, Dandri *et al.*[47] showed the effects of adefovir using uPA/scid mice repopulated with tupaia hepatocytes, which also support replication of human HBV. Oga *et al.*[48] identified a novel lamivudine-resistant variant that has an amino acid substitution outside of the YMDD motif. They showed that lamivudine was ineffective against the novel mutant strain. It is thus apparent that this mouse/human liver chimeric model is ideal to study the susceptibility of mutant strains to various drugs, because mutant viruses can easily be made and infected into chimeric mice.[13] The model has also been utilized to evaluate viral entry inhibitors derived from the large envelope protein.[49]

Study of hepatitis C virus using human hepatocyte chimeric mice

As observed in studies on HBV, HCV infection efficiency was poor and levels of viremia were low in mice where the repopulation rate of the mouse liver with human hepatocyte was low.[17,50] As shown in Figure 3, human albumin levels in mouse serum were significantly higher in mice in which measurable viremia developed (Hiraga *et al.* unpublished data). Recent studies have therefore been carried out using highly repopulated mice. The usefulness of a newly developed HCV assay,[51] and infectivity of a newly identified intergenotypic recombinant strain,[52] have been reported using the chimeric mice.

Using the remarkable replication ability of the JFH1 genotype 2a strain,[53] infectivity of JFH1 or intergenotypic chimeric viral particles, previously shown in cell culture, has now been shown to be infectious in chimeric mice.[54–56] Infectivity of viruses that were replicated in chimeric mice in cell culture has also been shown, and virus fitness has been studied.[55,56] The role of the HCV core+1 open reading frame and core *cis*-acting RNA elements has also been examined using the chimeric virus.[57] These elegant studies have the limitation that the non-structural part of the virus is limited to that of JFH1. Hiraga *et al.*[14] have shown that infectious clones of genotype 1a and JFH1 can be infected with direct injection of *in vitro* transcribed RNA into the mouse liver.[14] Similarly, Kimura *et al.*[15] reported the establishment of infectious clones of genotype 1b and ablation of RNA polymerase by site-directed mutagenesis abolish infectivity. These infectious clones will be useful for the study of drug-resistant strains.

The model of HCV infection has also been used to show that infection of the virus can be prevented by antibodies against

Table 1 New therapeutic strategies tested by human hepatocyte chimeric mice

n	Drug or cell	Strategy	Reference
1	Interferon alpha 2b	Activation of antiviral genes	Kneteman *et al.*[65]
	BILN-2061	NS3-4A protease inhibition	
	HCV371	NS5B polymerase inhibition	
2	Modified BID	Induction of apoptosis	Hsu *et al.*[66]
3	Serine palmitoyltransferase inhibitor	Disruption of lipid raft	Umehara *et al.*[67]
4	Lymphoblastoid interferon alpha	Activation of antiviral genes	Hiraga *et al.*[14]
5	Amphipathic DNA polymers	Blocking viral entry	Matsumura *et al.*[60]
6	Sec-butyl-analogue of HCV-371	NS5B polymerase inhibition	LaPorte *et al.*[68]
7	HCV796	NS5B polymerase inhibition	Kneteman *et al.*[69]
8	Liver allograft-derived lymphocyte	Adoptive immunotherapy	Ohira *et al.*[70]
9	Telaprevir	NS3-4A protease inhibition	Kamiya *et al.*[71]

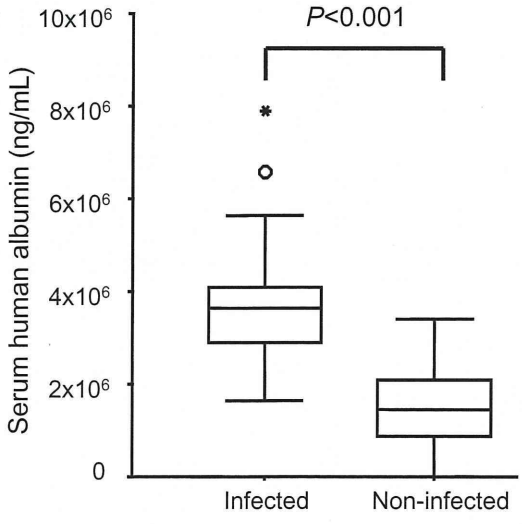

Figure 3 Human albumin levels in mice used in the hepatitis C virus (HCV) infection experiments. A total of 54 mice were injected with HCV positive serum samples containing 5×10^5 virus particles. A total of 24 mice became persistently positive for HCV-RNA, but 30 mice did not. Serum human albumin levels 2 weeks after human hepatocyte transplantation were compared between infected and non-infected mice.

CD81,[58] polyclonal human immunoglobulin directed to a similar strain,[59] and amphipathic DNA polymers.[60] Notably, the presence of broadly neutralizing antibodies to HCV that protect against heterologous viral infection has been reported, suggesting the possibility of a prophylactic vaccine against HCV.[61]

With respect to evasion of the virus against the innate immune response, altered intrahepatic expression profiles in the early phase of infection is of particular interest. The chimeric mice model is ideal for such studies; cross-hybridization of mouse and human can be avoided by careful experimental procedures.[62] Microarray analysis of livers of HCV infected and non-infected mice showed transcriptional activation of genes related to innate immune response, lipid metabolism, endoplasmic reticulum (ER) stress and apoptosis in HCV-infected mice.[63,64] The HCV infected mouse model is particularly useful for the study of newly developed HCV agents. The effect of recently developed chemicals and a unique therapy using intrahepatic lymphocytes have been shown using this model (Table 1). However, none of these therapies have yet been able to completely eradicate HCV from mice. It is noteworthy that ultra-rapid cardiotoxicity has been reported with the protease inhibitor BILN 2061 in the uPA/scid mice, but not in scid mice, implicating involvement of the uPA transgene.[72] Care should therefore be taken in interpreting the results obtained by this model.

Conclusion

Development of a small animal model using human hepatocyte chimeric mice has enabled us to study key aspects of HBV and HCV biology. The characteristic feature of the absence of human immune cells is suitable for studying viral replication and observing changes occurring in liver cells during viral infection, such as the innate immune response and cellular stress and metabolic responses. The model is also useful for studying the effect of drugs without the influence of cytokines and cytotoxic T lymphocytes. Nonetheless, the model is insufficient to study carcinogenesis of hepatitis viruses, because non-parenchymal cells in mouse liver are of mouse origin and do not support inflammation and fibrosis, which are probably closely related to carcinogenesis. The lack of human immune cells also limits the study of inflammation and immunity. Furthermore, the availability of human hepatocytes is limited. Despite these limitations, the current model shows great potential as a mouse model for the study of hepatitis viruses. Development of a small animal model with or without human immunity using stem cells or iPS cells would be an ideal model in the future.

Acknowledgments

This work was supported in part by Grants-in-Aid for scientific research and development from the Ministry of Education, Culture, Sports, Science and Technology, and the Ministry of Health, Labor and Welfare, Government of Japan.

References

1 Shepard CW, Simard EP, Finelli L, Flore AE, Bell BP. Hepatitis B virus infection: epidemiology and vaccination. *Epidemiol. Rev.* 2006; **28**: 112–25.

2 Sy T, Jamal MM. Epidemiology of Hepatitis C Virus (HCV) infection. *Int. J. Med. Sci.* 2006; **3**: 41–6.
3 Yuen MF, Hou JL, Chutaputti A, Prevent APWP. Hepatocellular carcinoma in the Asia pacific region. *J. Gastroenterol. Hepatol.* 2009; **24**: 346–53.
4 Guidotti LG, Matzke B, Schaller H, Chisari FV. High-level Hepatitis-B Virus-replication in transgenic mice. *J. Virol.* 1995; **69**: 6158–69.
5 Weber O, Schlemmer KH, Hartmann E *et al.* Inhibition of human hepatitis B virus (HBV) by a novel non-nucleosidic compound in a transgenic mouse model. *Antiviral Res.* 2002; **54**: 69–78.
6 Julander JG, Sidwell RW, Morrey JD. Characterizing antiviral activity of adefovir dipivoxil in transgenic mice expressing hepatitis B virus. *Antiviral Res.* 2002; **55**: 27–40.
7 Julander JG, Colonno RJ, Sidwell RW, Morrey JD. Characterization of antiviral activity of entecavir in transgenic mice expressing hepatitis B virus. *Antiviral Res.* 2003; **59**: 155–61.
8 Uprichard SL, Boyd B, Althage A, Chisari FV. Clearance of hepatitis B virus from the liver of transgenic mice by short hairpin RNA. *Proc. Natl. Acad. Sci U S A* 2005; **102**: 773–8.
9 Ilan E, Burakova T, Dagan S *et al.* The hepatitis B virus-trimera mouse: a model for human HBV infection and evaluation of Anti-HBV therapeutic agents. *Hepatology* 1999; **29**: 553–62.
10 Ilan E, Arazi J, Nussbaum O *et al.* The hepatitis C virus (HCV)-Trimera mouse: a model for evaluation of agents against HCV. *J. Infect. Dis.* 2002; **185**: 153–61.
11 Heckel JL, Sandgren EP, Degen JL, Palmiter RD, Brinster RL. Neonatal bleeding in transgenic mice expressing urokinase-type plasminogen-activator. *Cell* 1990; **62**: 447–56.
12 Rhim JA, Sandgren EP, Palmiter RD, Brinster RL. Complete reconstitution of mouse-liver with xenogeneic hepatocytes. *Proc. Natl. Acad Sci U S A* 1995; **92**: 4942–6.
13 Tsuge M, Hiraga N, Takaishi H *et al.* Infection of human hepatocyte chimeric mouse with genetically engineered hepatitis B virus. *Hepatology* 2005; **42**: 1046–54.
14 Hiraga N, Imamura M, Tsuge M *et al.* Infection of human hepatocyte chimeric mouse with genetically engineered Hepatitis C Virus and its susceptibility to interferon. *FEBS Lett.* 2007; **581**: 1983–7.
15 Kimura T, Imamura M, Hiraga N *et al.* Establishment of an infectious genotype 1b Hepatitis C Virus clone in human hepatocyte chimeric mice. *J.l Gen. Virol.* 2008; **89**: 2108–13.
16 Dandri M, Burda MR, Torok E *et al.* Repopulation of mouse liver with human hepatocytes and in vivo infection with hepatitis B virus. *Hepatology* 2001; **33**: 981–8.
17 Mercer DF, Schiller DE, Elliott JF *et al.* Hepatitis C virus replication in mice with chimeric human livers. *Nat. Med.* 2001; **7**: 927–33.
18 Douglas DN, Kawahara T, Sis B *et al.* therapeutic efficacy of human hepatocyte transplantation in a SCID/uPA mouse model with inducible liver disease. *PLoS ONE* 2010; **5**: e9209.
19 Tateno C, Yoshizane Y, Saito N *et al.* Near completely humanized liver in mice shows human-type metabolic responses to drugs. *Am. J. Pathol.* 2004; **165**: 901–12.
20 Bissig KD, Wieland SF, Tran P *et al.* Human liver chimeric mice provide a model for hepatitis B and C virus infection and treatment. *J. Clin. Invest.* 2010; **120**: 924–30.
21 Yu AM, Idle JR, Gonzalez FJ. Polymorphic cytochrome p450 2D6: humanized mouse model and endogenous substrates. *Drug. Metab. Rev.* 2004; **36**: 243–77.
22 Katoh M, Sawada T, Soeno Y *et al.* In vivo drug metabolism model for human cytochrome P450 enzyme using chimeric mice with humanized liver. *J. Pharm. Sci.-Us.* 2007; **96**: 428–37.
23 Katoh M, Matsui T, Nakajima M *et al.* In vivo induction of human cytochrome P450 enzymes expressed in chimeric mice with humanized liver. *Drug. Metab. Dispos.* 2005; **33**: 754–63.
24 Katoh M, Matsui T, Okumura H *et al.* Expression of human phase II enzymes in chimeric mice with humanized liver. *Drug. Metab. Dispos.* 2005; **33**: 1333–40.
25 Okumura H, Katoh M, Sawada T *et al.* Humanization of excretory pathway in chimeric mice with humanized liver. *Toxicol. Sci.* 2007; **97**: 533–8.
26 Shoda J, Okada K, Inada Y *et al.* Bezafibrate induces multidrug-resistance P-Glycoprotein 3 expression in cultured human hepatocytes and humanized livers of chimeric mice. *Hepatol. Res.* 2007; **37**: 548–56.
27 Petersen J, Burda MR, Dandri M, Rogler CE. Transplantation of human hepatocytes in immunodeficient UPA mice: a model for the study of hepatitis B virus. *Methods Mol. Med.* 2004; **96**: 253–60.
28 Yoshizato K, Tateno C. A human hepatocyte-bearing mouse: an animal model to predict drug metabolism and effectiveness in humans. *PPAR Res.* 2009; **2009**: 476217.
29 Yoshizato K, Tateno C, Utoh R. The mechanism of liver size control in mammals: a novel animal study. *Int. J. Design & Nature Ecodynamics* 2009; **4**: 123–42.
30 Utoh R, Tateno C, Yamasaki C *et al.* Susceptibility of chimeric mice with livers repopulated by serially subcultured human hepatocytes to hepatitis B virus. *Hepatology* 2008; **47**: 435–46.
31 Meuleman P, Leroux-Roels G. The human liver-uPA-SCID mouse: a model for the evaluation of antiviral compounds against HBV and HCV. *Antiviral Res.* 2008; **80**: 231–8.
32 Dandri M, Lutgehetmann M, Volz T, Petersen J. Small animal model systems for studying Hepatitis B Virus replication and pathogenesis. *Semin. Liver Dis.* 2006; **26**: 181–91.
33 Dandri M, Volz TK, Lutgehetmann M, Petersen J. Animal models for the study of HBV replication and its variants. *J. Clin. Virol.* 2005; **34** (Suppl. 1): S54–62.
34 Barth H, Robinet E, Liang TJ, Baumert TF. Mouse models for the study of HCV infection and virus-host interactions. *J. Hepatol.* 2008; **49**: 134–42.
35 Kneteman NM, Toso C. In vivo study of HCV in mice with chimeric human livers. *Methods Mol. Biol.* 2009; **510**: 383–99.
36 Meuleman P, Libbrecht L, De Vos R *et al.* Morphological and biochemical characterization of a human liver in a uPA-SCID mouse chimera. *Hepatology* 2005; **41**: 847–56.
37 Sugiyama M, Tanaka Y, Kato T *et al.* Influence of hepatitis B virus genotypes on the intra- and extracellular expression of viral DNA and antigens. *Hepatology* 2006; **44**: 915–24.
38 Tsuge M, Hiraga N, Akiyama R *et al.* HBx protein is indispensable for development of viremia in human hepatocyte chimeric mice. *J. Gen. Virol.* 2010.
39 Meuleman P, Libbrecht L, Wieland S *et al.* Immune suppression uncovers endogenous cytopathic effects of the hepatitis B virus. *J. Virol.* 2006; **80**: 2797–807.
40 Sugiyama M, Tanaka Y, Kurbanov F *et al.* Direct cytopathic effects of particular hepatitis B virus genotypes in severe combined immunodeficiency transgenic with urokinase-type plasminogen activator mouse with human hepatocytes. *Gastroenterology* 2009; **136**: 652–62.
41 Tanaka Y, Sanchez LV, Sugiyama M *et al.* Characteristics of Hepatitis B Virus genotype G coinfected with genotype H in chimeric mice carrying human hepatocytes. *Virology* 2008; **376**: 408–15.
42 Tatematsu K, Tanaka Y, Kurbanov F *et al.* A genetic variant of Hepatitis B Virus divergent from known human and ape genotypes isolated from a Japanese patient and provisionally assigned to new genotype J. *J. Virol.* 2009; **83**: 10538–47.
43 Tabuchi A, Tanaka J, Katayama K *et al.* Titration of Hepatitis B Virus infectivity in the sera of pre-acute and late acute phases of HBV infection: transmission experiments to chimeric mice with

human liver repopulated hepatocytes. *J. Med. Virol.* 2008; **80**: 2064–8.
44 Noguchi C, Imamura M, Tsuge M *et al.* G-to-A Hypermutation in Hepatitis B Virus (HBV) and clinical course of patients with chronic HBV infection. *J. Infect. Dis.* 2009; **199**: 1599–607.
45 Dandri M, Murray JM, Lutgehetmann M, Volz T, Lohse AW, Petersen J. Virion half-life in chronic hepatitis B infection is strongly correlated with levels of viremia. *Hepatology* 2008; **48**: 1079–86.
46 Hiraga N, Imamura M, Hatakeyama T *et al.* Absence of viral interference and different susceptibility to interferon between Hepatitis B Virus and Hepatitis C Virus in human hepatocyte chimeric mice. *J. Hepatol.* 2009; **51**: 1046–54.
47 Dandri M, Burda MR, Zuckerman DM *et al.* Chronic infection with Hepatitis B Viruses and antiviral drug evaluation in uPA mice after liver repopulation with tupaia hepatocytes. *J. Hepatol.* 2005; **42**: 54–60.
48 Yatsuji H, Noguchi C, Hiraga N *et al.* Emergence of a novel lamivudine-resistant hepatitis B virus variant with a substitution outside the YMDD motif. *Antimicrob. Agents Chemother.* 2006; **50**: 3867–74.
49 Petersen J, Dandri M, Mier W *et al.* Prevention of Hepatitis B Virus infection in vivo by entry inhibitors derived from the large envelope protein. *Nat. Biotechnol.* 2008; **26**: 335–41.
50 Turrini P, Sasso R, Germoni S *et al.* Development of humanized mice for the study of hepatitis C virus infection. *Transplant. Proc.* 2006; **38**: 1181–4.
51 Cagnon L, Wagaman P, Bartenschlager R *et al.* Application of the trak-C (TM) HCV core assay for monitoring antiviral activity in HCV replication systems. *J. Virol. Methods* 2004; **118**: 23–31.
52 Kurbanov F, Tanaka Y, Chub E *et al.* Molecular epidemiology and interferon susceptibility of the natural recombinant Hepatitis C Virus Strain RF1-2k/1b. *J. Infect. Dis.* 2008; **198**: 1448–56.
53 Wakita T, Pietschmann T, Kato T *et al.* Production of infectious hepatitis C virus in tissue culture from a cloned viral genome. *Nat. Med.* 2005; **11**: 791–6.
54 Grove J, Huby T, Stamataki Z *et al.* Scavenger receptor BI and BII expression levels modulate Hepatitis C Virus infectivity. *J. Virol.* 2007; **81**: 3162–9.
55 Lindenbach BD, Meuleman P, Ploss A *et al.* Cell culture-grown Hepatitis C Virus is infectious in vivo and can be recultured in vitro. *Proc. Natl. Acad. Sci. U S A* 2006; **103**: 3805–9.
56 Kaul A, Woerz I, Meuleman P, Leroux-Roels G, Bartenschlager R. Cell culture adaptation of Hepatitis C Virus and in vivo viability of an adapted variant. *J. Virol.* 2007; **81**: 13168–79.
57 Vassilaki N, Friebe P, Meuleman P *et al.* Role of the Hepatitis C Virus Core+1 open reading frame and core cis-acting RNA Elements in Viral RNA translation and replication. *J. Virol.* 2008; **82**: 11503–15.
58 Meuleman P, Hesselgesser J, Paulson M *et al.* Anti-CD81 antibodies can prevent a Hepatitis C Virus infection in vivo. *Hepatology* 2008; **48**: 1761–8.
59 Vanwolleghem T, Bukh J, Meuleman P *et al.* Polyclonal immunoglobulins from a chronic Hepatitis C Virus patient protect human liver-chimeric mice from infection with a homologous Hepatitis C Virus strain. *Hepatology* 2008; **47**: 1846–55.
60 Matsumura T, Hu ZY, Kato T *et al.* Amphipathic DNA polymers inhibit Hepatitis C Virus infection by blocking viral entry. *Gastroenterology* 2009; **137**: 673–81.
61 Law M, Maruyama T, Lewis J *et al.* Broadly neutralizing antibodies protect against Hepatitis C Virus quasispecies challenge. *Nat. Med.* 2008; **14**: 25–7.
62 Walters KA, Joyce MA, Thompson JC *et al.* Application of functional genomics to the chimeric mouse model of HCV infection: optimization of microarray protocols and genomics analysis. *Virol. J.* 2006; **3**: 37–44.
63 Walters KA, Joyce MA, Thompson JC *et al.* Host-specific response to HCV infection in the chimeric SCID-beige/Alb-uPA mouse model: role of the innate antiviral immune response. *PLoS Pathog.* 2006; **2**: 591–602.
64 Joyce MA, Walters KA, Lamb SE *et al.* HCV Induces Oxidative and ER Stress, and Sensitizes Infected Cells to Apoptosis in SCID/Alb-uPA Mice. *PLoS Pathog.* 2009; **5**: e10000291.
65 Kneteman NM, Weiner AJ, O'Connell J *et al.* Anti-HCV therapies in chimeric scid-Alb/uPA mice parallel outcomes in human clinical application. *Hepatology* 2006; **43**: 1346–53.
66 Hsu EC, Hsi B, Hirota-Tsuchihara M *et al.* Modified apoptotic molecule (BID) reduces hepatitis C virus infection in mice with chimeric human livers. *Nat. Biotechnol.* 2003; **21**: 519–25.
67 Umehara T, Sudoh M, Yasui F *et al.* Serine palmitoyltransferase inhibitor suppresses HCV replication in a mouse model. *Biochem. Biophys. Res. Commun.* 2006; **346**: 67–73.
68 Laporte MG, Jackson RW, Draper TL *et al.* The discovery of pyrano[3,4-b]indole-based allosteric inhibitors of HCV NS5B polymerase with in vivo activity. *Med. Chem.* 2008; **3**: 1508–15.
69 Kneteman NM, Howe AYM, Gao TJ *et al.* HCV796: a selective nonstructural protein 5B polymerase inhibitor with potent Anti-Hepatitis C Virus activity in vitro, in mice with chimeric human livers, and in humans infected with Hepatitis C Virus. *Hepatology* 2009; **49**: 745–52.
70 Ohira M, Ishiyama K, Tanaka Y *et al.* Adoptive immunotherapy with liver allograft-derived lymphocytes induces anti-HCV activity after liver transplantation in humans and humanized mice. *J. Clin. Invest.* 2009; **119**: 3226–35.
71 Kamiya N, Iwao E, Hiraga N *et al.* Practical Evaluation of a Mouse with Chimeric Human Liver Model for Hepatitis C Virus Infection Using an NS3-4A Protease Inhibitor. *J. Gen. Virol.* 2010; **91**: 1668–77.
72 Vanwolleghem T, Meuleman P, Libbrecht L *et al.* Ultra-rapid cardiotoxicity of the hepatitis C virus protease inhibitor BILN 2061 in the urokinase-type plasminogen activator mouse. *Gastroenterology* 2007; **133**: 1144–55.

Journal of General Virology (2010), 91, 1668–1677 DOI 10.1099/vir.0.019315-0

Practical evaluation of a mouse with chimeric human liver model for hepatitis C virus infection using an NS3-4A protease inhibitor

Naohiro Kamiya,[1] Eiji Iwao,[1] Nobuhiko Hiraga,[2,3] Masataka Tsuge,[2,3] Michio Imamura,[2,3] Shoichi Takahashi,[2,3] Shinji Miyoshi,[4] Chise Tateno,[3,5] Katsutoshi Yoshizato[3,5] and Kazuaki Chayama[2,3]

Correspondence
Kazuaki Chayama
chayama@hiroshima-u.ac.jp

[1]Pharmacology Department V, Mitsubishi Tanabe Pharma Corporation, Yokohama, Japan

[2]Department of Medicine and Molecular Science, Division of Frontier Medical Science, Programs for Biomedical Research, Graduate School of Biomedical Sciences, Hiroshima University, Hiroshima, Japan

[3]Liver Research Project Center, Hiroshima University, Hiroshima, Japan

[4]DMPK Department, Mitsubishi Tanabe Pharma Corporation, Kisarazu, Chiba, Japan

[5]PhoenixBio, Higashihiroshima, Japan

A small-animal model for hepatitis C virus (HCV) infection was developed using severe combined immunodeficiency (SCID) mice encoding homozygous urokinase-type plasminogen activator (uPA) transplanted with human hepatocytes. Currently, limited information is available concerning the HCV clearance rate in the SCID mouse model and the virion production rate in engrafted hepatocytes. In this study, several cohorts of $uPA^{+/+}/SCID^{+/+}$ mice with nearly half of their livers repopulated by human hepatocytes were infected with HCV genotype 1b and used to evaluate HCV dynamics by pharmacokinetic and pharmacodynamic analyses of a specific NS3-4A protease inhibitor (telaprevir). A dose-dependent reduction in serum HCV RNA was observed. At telaprevir exposure equivalent to that in clinical studies, rapid turnover of serum HCV was also observed in this mouse model and the estimated slopes of virus decline were 0.11–0.17 $\log_{10}$ h^{-1}. During the initial phase of treatment, the $\log_{10}$ reduction level of HCV RNA was dependent on the drug concentration, which was about fourfold higher in the liver than in plasma. HCV RNA levels in the liver relative to human endogenous gene expression were correlated with serum HCV RNA levels at the end of treatment for up to 10 days. A mathematical model analysis of viral kinetics suggested that 1 g of the chimeric human liver could produce at least 10^8 virions per day, and this may be comparable to HCV production in the human liver.

Received 17 December 2009
Accepted 17 February 2010

INTRODUCTION

Hepatitis C virus (HCV) is a major cause for concern worldwide. More than 3 % of the world's population is chronically infected with HCV and 3–4 million people are newly infected each year (Wasley & Alter, 2000). Chronic HCV infection is relatively mild and progresses slowly; however, about 20 % of chronic hepatitis C (CHC) carriers progress to serious end-stage liver disease (Lauer & Walker, 2001; Liang *et al.*, 2000; Poynard *et al.*, 2003). The current standard treatment for HCV infection is administration of pegylated alpha interferon (PEG-IFN) in combination with ribavirin (RBV) for 48 weeks. The overall cure rates with this intervention are 40–50 % for patients with genotype 1 and more than 75 % for patients with genotypes 2 and 3 (Fried *et al.*, 2002; Manns *et al.*, 2001). Several compounds that inhibit specific stages of the virus life cycle have been clinically evaluated (Manns *et al.*, 2007; Pereira & Jacobson, 2009). Telaprevir is a novel peptidomimetic slow- and tight-binding inhibitor of HCV NS3-4A protease, which was discovered using a structure-based drug design approach (Perni *et al.*, 2006). A rapid decline in viral RNA was observed in CHC patients treated with telaprevir (Reesink *et al.*, 2006) and an increased antiviral effect of a combination of telaprevir and PEG-IFN has been reported (Forestier *et al.*, 2007). Recent clinical trials of telaprevir in combination with PEG-IFN and RBV have indicated a promising material advance in therapy for CHC patients (Hézode *et al.*, 2009; McHutchison *et al.*, 2009). First-generation HCV-specific agents have been developed despite the lack of small-animal models for HCV infection. However, early emergence of resistant variants against novel antiviral agents is a concern. Thus, the use of two or more investigation agents is strongly recommended for

clinical studies in CHC patients (Sherman *et al.*, 2007). To ensure ethical and safe clinical trials, animal models continue to be necessary for the mechanistic evaluation of the ability of specific agents to inhibit the virus life cycle *in vivo* and to develop better therapeutic strategies, including combination regimens (Boonstra *et al.*, 2009). Several groups have developed a small-animal model for HCV infection using homozygous urokinase-type plasminogen activator (uPA)/severe combined immunodeficiency (SCID) ($uPA^{+/+}$/$SCID^{+/+}$) mice transplanted with human hepatocytes (Mercer *et al.*, 2001). These mice are susceptible to cell culture-grown HCV (HCVcc; Lindenbach *et al.*, 2006) and have been used to evaluate antiviral agents including IFN-α, BILN 2061 (an NS3-4A protease inhibitor) and HCV796 (an NS5B polymerase inhibitor) (Kneteman *et al.*, 2006, 2009; Vanwolleghem *et al.*, 2007). However, the HCV clearance rate in the SCID mouse model and the virion production rate in hepatocytes engrafted in the mouse liver are not fully understood. We also generated a mouse model with an almost humanized liver (Tateno *et al.*, 2004). Using this mouse model, we reported the infection of a genetically engineered hepatitis B virus (Tsuge *et al.*, 2005) and developed a reverse genetics system for HCV genotypes 1a, 1b and 2a after intrahepatic injection of *in vitro*-transcribed RNA as well as intravenous injection of HCVcc (Hiraga *et al.*, 2007; Kimura *et al.*, 2008). In this study, we demonstrated the rapid turnover of serum HCV RNA and the pharmacokinetics (PK) and pharmacodynamics (PD) of telaprevir treatment. We concluded after quantitative estimation and the use of a mathematical model that HCV production equivalent to that in the human liver is possible in engrafted hepatocytes in this mouse model.

RESULTS

Preliminary dose-finding study

At the beginning of this study, we attempted to determine an effective dose regimen for telaprevir in this mouse model. Nine mice were randomized and treated with telaprevir over three time periods (Table 1). The lifetime kinetics of serum HCV RNA and of human serum albumin (HSA) in blood are represented in Fig. 1. One mouse (A07) exhibited a rapid reduction in HSA in the blood, which indicated the instability of human hepatocyte grafts. As a rapid reduction in HSA levels was not observed in subsequent experiments, this mouse was excluded from the mean analysis. After 7 days of twice daily (BID) dosing in period 1, the mean $\log_{10}$ changes in HCV RNA from baseline ($\pm$SEM) after the 100 and 10 mg telaprevir kg^{-1} doses were -0.49 ± 0.094 and -0.53 ± 0.039, respectively, and no dose-dependent reduction was observed. During period 2, the dose frequency was changed from BID to three times daily (TID), and the time of serum sampling was also changed from 1 to 4 h after the last dose. After the 3-day treatment, the mean $\log_{10}$ changes of HCV RNA in 100 and 10 mg telaprevir kg^{-1} TID groups were -1.00 ± 0.166 and -0.28 ± 0.056, respectively, and the difference between the two groups was significant. To test the reproducibility of results, mice were treated with 10 or 100 mg telaprevir kg^{-1} TID for 10 days and then sacrificed 5 h after the administration of the last dose. The mean $\log_{10}$ changes in serum HCV RNA were -1.46 ± 0.265 and -0.27 ± 0.073 in the 100 and 10 mg kg^{-1} TID groups, respectively, and the difference between the means was significant.

Evaluation of HCV turnover in this mouse model

Because of the SCID nature of this mouse model, the virion clearance mechanism was of interest. Six mice with steady-state and high viral loads (9.7×10^5–1.2×10^8 copies ml^{-1}) were administered 200 mg telaprevir kg^{-1} TID for 4 days, with 5 h intervals between doses and a 14 h intermission from drug treatment each day. Because the $\log_{10}$ reduction in HCV RNA appeared to depend on the time of serum collection during the day (Fig. 2a), the mean $\log_{10}$ changes in HCV RNA were plotted against time and fitted to a linear regression model (Fig. 2b). The estimated slopes (i.e. $\log_{10}$ HCV reduction per hour) and 95% confidence intervals (CI) on days 1, 2 and 3 were -0.165 (-0.268 to 0.0616), -0.115 (-0.131 to 0.0990) and -0.153, respectively. These regression lines also suggested that extrapolated HCV loads at the actual times of the daily first doses were 0.0530, -0.220 and -0.0948 $\log_{10}$ copies ml^{-1}, respectively. Therefore, it appeared that the viral load

Table 1. Telaprevir dose-finding experiment

Period	Duration (days)	Frequency of dose (per day)	Dose (mg kg^{-1})	No. of mice	Mean $\log_{10}$ changes $\pm$ SEM	*P* value (*t* test)
1	7	2	100	4	-0.49 ± 0.094	0.7806
			10	3*	-0.53 ± 0.039	
			0	1	-0.47	
2	3	3	100	4*	-1.00 ± 0.166	0.0064
			10	4	-0.28 ± 0.056	
3	10	3	100	3	-1.46 ± 0.265	0.0125
			10	3	-0.27 ± 0.073	

*One mouse was excluded because of instability of human hepatocyte grafts.

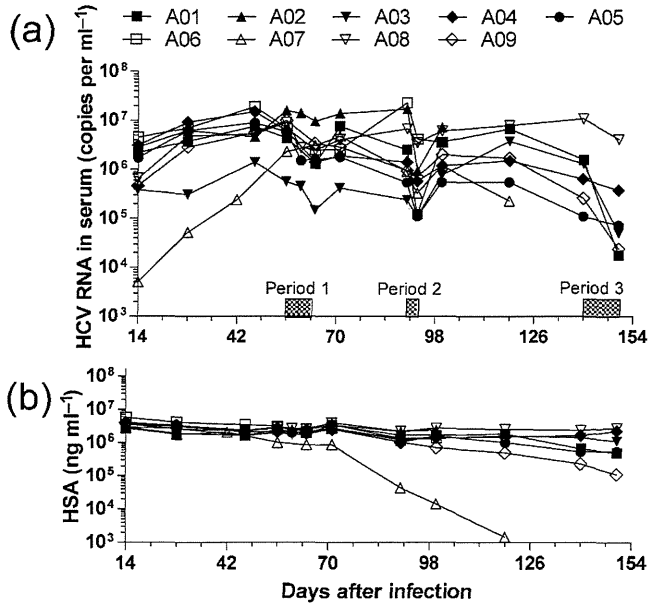

Fig. 1. Lifelong changes in serum HCV RNA and HSA in the blood of HCV-infected mice in the preliminary dose-finding experiment. Nine HCV-infected mice (A01–A09) were treated with telaprevir over three independent periods. The mice were treated with 10 mg telaprevir kg^{-1}, 100 mg telaprevir kg^{-1} or vehicle BID for 7 days (period 1), TID for 3 days (period 2) and TID for 10 days (period 3). (a) Kinetics of serum HCV RNA. (b) Kinetics of HSA level in blood. Because the HSA level indicated the stability of engrafted human hepatocytes in the mice, mouse A07 was excluded from the summary of the results in Table 1.

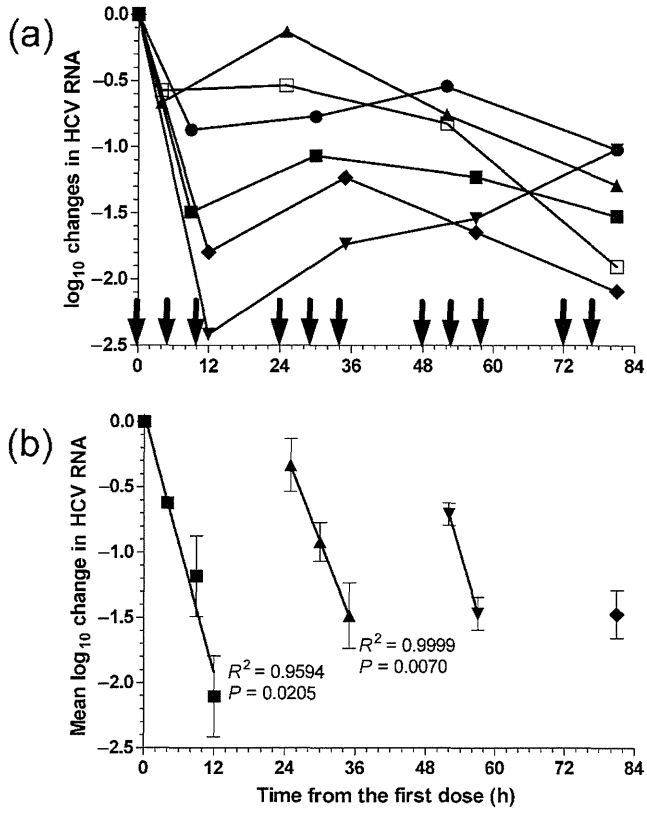

Fig. 2. Estimation of virus clearance rate. Six HCV-infected mice were treated with 200 mg telaprevir kg^{-1} TID for 4 days. Individual kinetics of $\log_{10}$ reductions in serum HCV RNA (a) and of mean $\log_{10}$ changes (±SEM) at each sampling time (b) are represented. Arrows indicate the times of dosing. The slopes of mean $\log_{10}$ HCV RNA reduction were estimated by linear regression analysis. P and R^2 values are indicated on the figure.

reverted back towards baseline levels during the 14 h intermission from drug treatment.

PK analysis

To assess drug exposure after repeated dosing in this mouse model, mice were administered 100 or 300 mg telaprevir kg^{-1} BID for 4 days. The mice receiving 300 mg kg^{-1} BID for 4 days had a mean 2 $\log_{10}$-fold HCV reduction, whereas those receiving 100 mg kg^{-1} BID had up to a 1.5 $\log_{10}$-fold reduction by day 3 (Fig. 3a). Plasma telaprevir concentrations after administration of the final dose are indicated in Fig. 3(b). The estimated half-life of telaprevir in the 100 and 300 mg kg^{-1} groups was 2.4 and 3.8 h, respectively.

PK/PD analysis and the dose-dependent reduction in HCV RNA

To evaluate the correlation between telaprevir concentration and HCV reductions in this mouse model, we used another cohort of 12 HCV-infected mice with high viral loads (1.6×10^6–3.9×10^8 copies ml^{-1}). In this crossover study, mice were randomized into three groups (n=4 each), each of which underwent two periods of dosing for 5 days separated by a 1-week washout period. Serum and plasma samples were collected once daily 5 h after dosing. The mean $\log_{10}$ changes in HCV RNA (±SEM) at different dose levels were calculated from the combined results of both periods (Fig. 4a). The mean $\log_{10}$ reductions from baseline in the 100 and 300 mg kg^{-1} groups were approximately 1 $\log_{10}$ and 1.5–2 $\log_{10}$, respectively, and the difference between the two groups was statistically significant. The means calculated in each period separately are also shown in Fig. 4(b). The plasma telaprevir concentration was positively correlated with the $\log_{10}$ HCV RNA reduction level in each period (Fig. 4c).

Drug concentrations and HCV levels in blood correlate with those in the liver

The correlation between telaprevir concentrations in the plasma and liver was analysed in a double logarithmic plot 5 (dose-finding cohort) or 8 h (PK and PK/PD cohorts) after the last dose (Fig. 5). The linear regression lines suggested that telaprevir concentrations in the liver were 5–

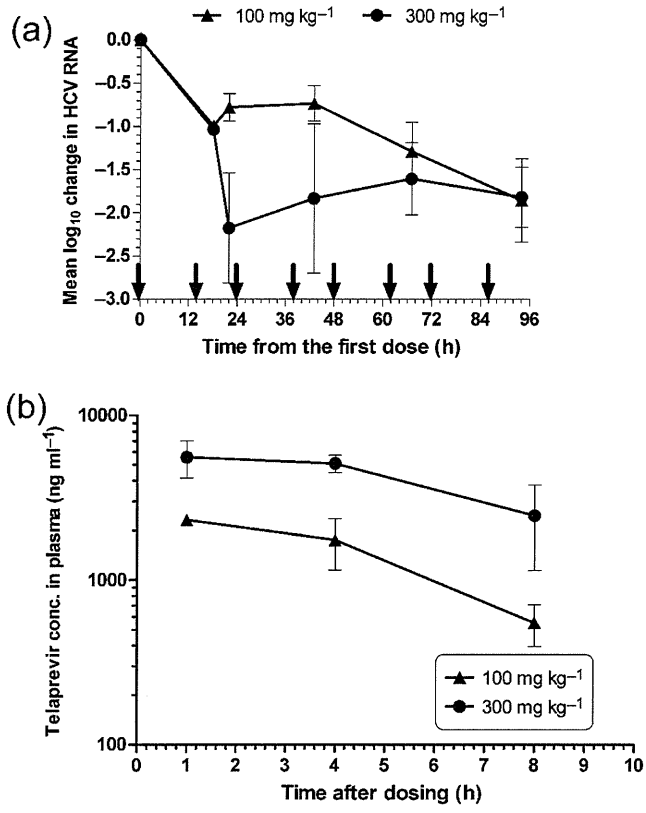

Fig. 3. PK analysis of telaprevir in the HCV-infected mouse model. Six HCV-infected mice were administered 100 (n=3) or 300 (n=3) mg telaprevir kg^{-1} BID for 4 days and serum samples were collected once daily to assess antiviral activity. After the last dose, plasma samples were collected at 1, 4 and 8 h for PK analysis. (a) Mean $\log_{10}$ changes (± SEM) in serum HCV RNA from mice treated with telaprevir. Arrows indicate the times of dosing. (b) Kinetics of telaprevir concentrations in plasma after the last dose.

10-fold higher at 5 h and approximately fourfold higher at 8 h than those in plasma. Total cellular RNA samples were extracted from two, one and four discrete small sections (approx. 50 mg) of the liver in the preliminary dose-finding, PK and PK/PD cohorts, respectively. HCV RNA levels in the total cellular RNA extract were relatively quantified by duplex real-time RT-PCR analysis using human β_2-microglobulin (hβ_2m) as an internal standard of human endogenous gene expression. Neither the threshold cycle (Ct) of hβ_2m ($Ct_{h\beta 2m}$) nor the Ct of HCV (Ct_{HCV}) correlated with total RNA from a small section of the chimeric human livers (data not shown). This result indicated that occupancy rates of human cells varied individually and/or among small sections of the chimeric human liver. Therefore, the mean difference in Ct ($\Delta Ct = Ct_{HCV} - Ct_{h\beta 2m}$) in each mouse was calculated and plotted against the viral load in serum (Fig. 6). After treatment with telaprevir for up to 10 days, mean ΔCt values ranged between 11 (HCV RNA content: $2^{11} = 2 \times 10^3$-fold lower than hβ_2m expression) and 17 (1×10^5-fold lower) among the HCV-infected mice and correlated linearly with $\log_{10}$ serum HCV RNA levels.

Viral dynamics model analysis

To evaluate time-dependent reductions in HCV with BID dosing, 12 HCV-infected elderly mice, which maintained high and steady-state viral loads (1.2×10^6–8.5×10^7 copies ml^{-1}) for more than 6 months, were treated with 200 mg telaprevir kg^{-1} BID for 3 days. The mice were divided into two groups, and serum samples were collected just before the second dose and 4 (n=6) or 8 (n=6) h after every two administrations. The single administration of telaprevir resulted in a mean 0.8–1.0 $\log_{10}$-fold reduction in HCV RNA in both groups. After the second dose, the pattern of viral kinetics appeared to depend on the time of serum collection, and the mean HCV RNA reduction level was higher in the 8 h group than in the 4 h group and plateaued at approximately a 2 $\log_{10}$-fold reduction in both groups after treatment for 3 days (Fig. 7). Finally, we attempted to estimate parameters of efficacy (ε) and virus clearance (c) per hour in this mouse model for comparison with estimates derived from human studies. Because the mean viral kinetics of the 8 h group was biphasic, the values in the 8 h group were used together for the mathematical model analysis. The estimated ε and c values were 0.992 (95 % CI 0.982–1.00) and 0.200 (95 % CI 0.110–0.291), respectively.

DISCUSSION

Using a mouse model with a chimeric human liver for HCV infection, we analysed the PK/PD of telaprevir treatment and investigated HCV dynamics during the initial phase of protease inhibitor treatment. All the mice in this study were expected to have more than half of their livers repopulated by human hepatocytes (Tateno *et al.*, 2004), which simulates a human drug metabolism profile (Katoh *et al.*, 2007, 2008). After the infection with HCV genotype 1b, high viral loads were maintained in the mice for more than 6 months. Recent studies have indicated the utility of a human/mouse chimera model for HCV infection to evaluate antiviral efficacy (Kneteman *et al.*, 2006, 2009) and preclinical safety (Vanwolleghem *et al.*, 2007). However, PK/PD studies and estimations of virus clearance rate have rarely been performed in this mouse model. HCV production, including intracellular replication in engrafted hepatocytes, has also not yet been elucidated. Despite the SCID nature of this mouse model, a 2 $\log_{10}$-fold HCV RNA reduction was observed within 0.5 days, as has been observed previously in CHC patients (Forestier *et al.*, 2007; Reesink *et al.*, 2006). In this mouse model, the rapid rebound in HCV load during the intermission from drug exposure indicated the rapid production and release of HCV into the circulation. This finding indicates that a virion-clearing compartment, which does not depend on T- and B-cell responses, may exist in this mouse model.

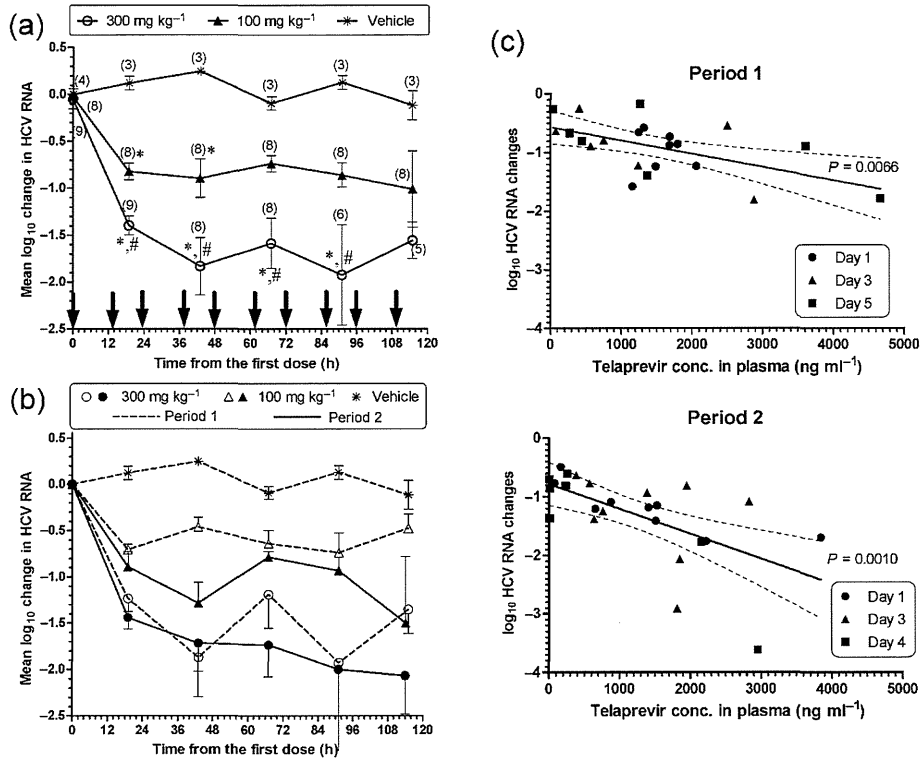

Fig. 4. PK/PD analysis and the dose-dependent reduction in HCV. Twelve HCV-infected mice were randomized into three groups (n=4 each) and then underwent two periods of telaprevir BID dosing for 5 days, separated by a 1-week washout period. Before the second period, the mice in the vehicle control group were additionally assigned to active drug groups. During the second period, mice that received the high or low doses were crossed over to the alternative treatment. Serum and plasma samples were collected once daily 5 h after dosing. Mean $\log_{10}$ changes (± SEM) in serum HCV RNA were calculated from the combined results from both periods (a) and each period separately (b). Arrows indicate the times of dosing. *, $P<0.05$ versus vehicle control group; #, $P<0.05$ versus 100 mg kg^{-1} group. (c) Correlation between $\log_{10}$ reduction in serum HCV and telaprevir concentrations in plasma. Linear regressions (solid lines) and 95 % CI (dashed lines) are indicated.

One possible explanation is that viral kinetics after liver transplantation in humans may play a role in HCV clearance under immunosuppressed conditions (Dahari *et al.*, 2005; Powers *et al.*, 2006; Schiano *et al.*, 2005). This observation suggests that this mouse model is capable of evaluating 'first-phase' HCV clearance after drug treatment.

In a clinical trial of telaprevir, CHC patients who exhibited a continuous decline in viral kinetics had mean plasma trough levels above 1000 ng ml^{-1}; therefore, a dose of 750 mg TID was selected for further clinical studies (Sarrazin *et al.*, 2007). When HCV-infected mice were administered 100 or 300 mg telaprevir kg^{-1}, a plasma concentration above 1000 ng ml^{-1} was maintained beyond 8 h in mice treated with 300 mg kg^{-1} but not in those treated with 100 mg kg^{-1}. This result suggests that the extrapolation of telaprevir doses from this mouse model to human studies depends on body surface area, i.e. approximately 15th of a dose in this mouse model may be equivalent to a dose in humans. In another cohort of mice treated with 100 and 300 mg telaprevir kg^{-1} BID, a dose-dependent reduction in HCV was observed and the plasma telaprevir concentration correlated significantly with the HCV reduction level. Therefore, the PK/PD results in this mouse model may be able to indicate a targeted dose range in clinical studies.

Whereas a telaprevir concentration in plasma equivalent to its dosage in clinical trials was achieved in this mouse model, the serum HCV RNA level plateaued at a decrease of approximately 2 $\log_{10}$-fold within several days of treatment. A saturated reduction of approximately 2 $\log_{10}$-fold after treatments with BILN 2061 and IFN was also reported in an analogous mouse model (Kneteman *et al.*, 2006; Vanwolleghem *et al.*, 2007). These observations led us to examine HCV replication in the chimeric human liver. In the relative quantification of HCV RNA against human-specific endogenous gene expression, we observed a correlation between the serum HCV RNA level and the mean ΔCt value in the liver, despite no correlation between the total RNA concentration and each Ct value of two target genes in the liver RNA extracts. This result can be interpreted to indicate that HCV replicated only in

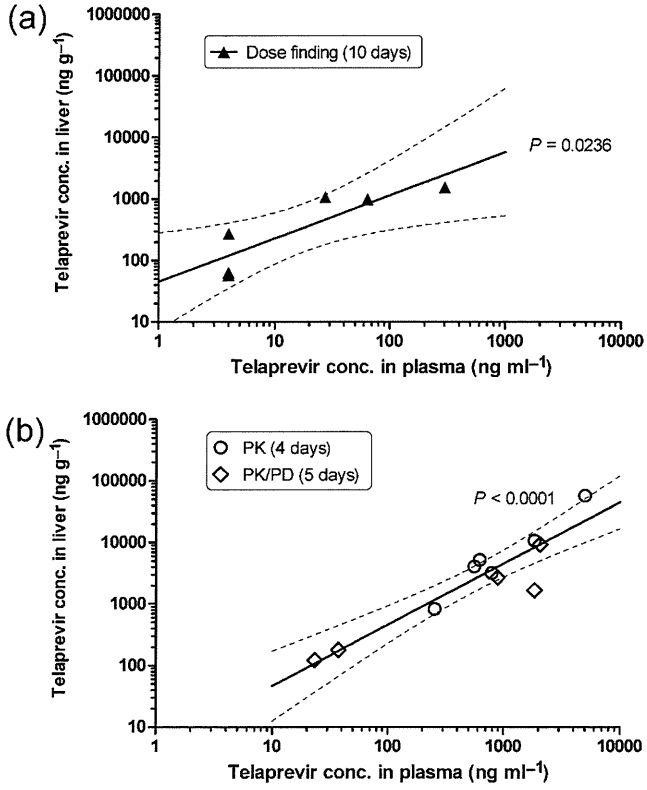

Fig. 5. Correlation between telaprevir concentrations in the liver and plasma. Telaprevir concentrations in the liver and plasma were determined at the end of the three different experiments indicated in Fig. 1 (dose-finding), Fig. 3 (PK) and Fig. 4 (PK/PD). Telaprevir concentrations in the liver were plotted against those in plasma 5 (a) or 8 (b) h after the last dose. Linear regressions (solid lines) and 95 % CI (dashed lines) are indicated.

engrafted human hepatocytes, and the observed HCV reduction in serum might reflect virus replication in the human hepatocyte grafts. Moreover, the relative content of HCV RNA was 2×10^3–1×10^5-fold lower than hβ_2m expression, whereas an HCV replicon cell line, which had approximately 1000 replicon genomes per cell (Quinkert *et al.*, 2005), contained nearly equal amounts of both genes (data not shown). HCV replication was much lower in the engrafted human hepatocytes than in an HCV replicon cell line, and HCV infected only a small portion of the engrafted human hepatocytes. It has been reported that 4–25 % of hepatocytes in a CHC patient were positive for replicative-intermediate RNA, and the mean number of viral genomes per productively infected hepatocyte ranged from 7 to 64 molecules (Chang *et al.*, 2003). Also, a more recent report suggested that the percentage of HCV antigen-positive hepatocytes in patients varied from 0 to 40 %, and the HCV content in 2000 microdissected HCV-positive cells ranged from 40 to 1800 international units using a branched DNA assay (Vona *et al.*, 2004). Therefore, we suggest that HCV replication efficiency in engrafted human hepatocytes is equivalent to that in CHC patients.

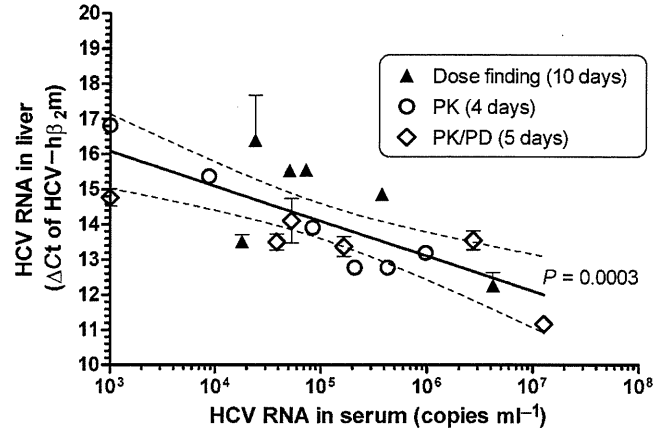

Fig. 6. Correlation between HCV content in the liver and serum. Relative quantification of HCV RNA levels in the liver was determined by the difference between threshold cycles (ΔCt) of HCV RNA and hβ_2m in a duplex real-time RT-PCR analysis. Linear regressions (solid line) and 95 % CI (dashed lines) are indicated.

The differences observed between the engrafted human hepatocytes and the HCV replicon cell line can be explained by the following assumptions: approximately 10 % of engrafted human hepatocytes are productively

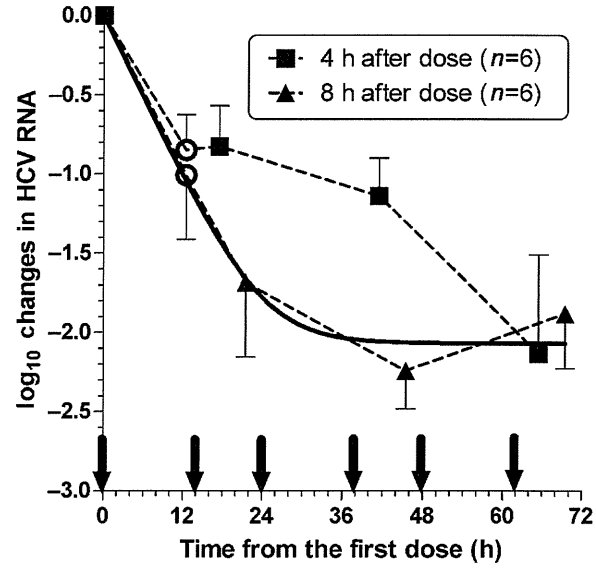

Fig. 7. Viral dynamics under BID telaprevir treatment. Mice were administered 200 mg telaprevir kg^{-1} BID at the times indicated by arrows. Serum samples were collected just before the second dose was administered and 4 (n=6) or 8 (n=6) h after every two doses were administered. Mean $\log_{10}$ changes (±SEM) in serum HCV RNA are plotted. The solved equation described in Methods was fitted to the values in the 8 h group (solid line), and the estimated efficacy and virion clearance rates were 0.992 (95 % CI 0.982–1.00) and 0.200 (95 % CI 0.110–0.291), respectively.

infected and harbour approximately ten HCV genomes per cell at baseline steady state and a 2 $\log_{10}$-fold reduction is achieved with drug treatment.

Mathematical models have proven valuable in understanding the *in vivo* dynamics of HCV, and very rapid dynamic processes occur on timescales of hours to days, and slower processes occur on timescales of weeks to months (Perelson & Ribeiro, 2008). In the last experiment, we observed a biphasic decline in the HCV RNA level after BID dosing for 3 days. During the first 2 days of the treatment, a discrepancy in viral kinetics between the serum-sampling time points was noted. Similarly, fluctuations in viral kinetics during the first-phase slope were observed in patients who received IFN three times a week (Pawlotsky *et al.*, 2004). Variable efficacy rate determined by PK parameters can explain fluctuations during the first-phase slope in mathematical model analysis (Talal *et al.*, 2006). However, it is difficult to evaluate the individual temporal changes in viral and drug kinetics using a mouse model as only a limited volume of blood is available for analysis. Therefore, we assumed a constant efficacy rate (ε) and omitted a turnover rate of hepatocytes because of the short duration of treatment. The estimated clearance rate (c) in this study was 4.8 day^{-1}. Additionally, the mean slope of 0.144 $\log_{10}$ h^{-1} (Fig. 2b) could be transformed to 0.332 h^{-1}=8.0 day^{-1} according to the change of base of a logarithm. The estimated clearance rates in this mouse model basically agreed with estimates determined in humans infected with HCV genotype 1 and undergoing IFN-based therapies (Herrmann *et al.*, 2003; Neumann *et al.*, 1998; Pawlotsky *et al.*, 2004) or large-volume plasma apheresis (Ramratnam *et al.*, 1999). Total virion production during steady-state viral kinetics in this mouse model was calculated by multiplying c by the initial viral load (V_0) and then normalizing the extracellular fluid volume. From previous studies, it was determined that 10^{11}–10^{13} virions are produced daily in patients with high HCV loads (Neumann *et al.*, 1998; Ramratnam *et al.*, 1999). In this mouse model, the volume of extracellular fluid and weight of the liver were approximately 20 and 9 % of the body weight (data not shown), and the mean $\log_{10}$ V_0 ($\pm$SEM) among the mice with mean clearance rates of 4.8 and 8.0 per day were 6.96$\pm$0.26 and 7.00$\pm$0.33, respectively. The results of the calculations indicated that 1 g of the chimeric human liver produced 1×10^8–2×10^8 virions per day. The typical weight of the human liver is 1–2 kg; thus, the capacity of human hepatocytes to produce HCV in this mouse model may be equivalent to that in CHC patients. In conclusion, a mouse model with a chimeric human liver can simulate HCV replication in human patients quantitatively and dynamically, and this mouse model may be suitable for preclinical evaluations of novel HCV-specific agents and other therapeutic strategies, including combination regimens.

METHODS

Generation of mice with chimeric human livers and HCV infection. The generation of uPA$^{+/+}$/SCID$^{+/+}$ mice and transplantation of frozen human hepatocytes was performed at PhoenixBio. Graft function was monitored on the basis of HSA levels in blood (Tsuge *et al.*, 2005). All the mice had high HSA levels, which suggested that nearly half of their livers were repopulated by human hepatocytes (Tateno *et al.*, 2004). After obtaining written informed consent, we collected sera periodically from patients who were chronically infected with HCV genotype 1b and failed to respond to PEG-IFN and RBV therapy. The mice were inoculated with the serum samples via the orbital vein after anaesthetization. The experimental protocol was approved by the Ethics Review Committee for Animal Experimentation of the Graduate School of Biomedical Sciences, Hiroshima University.

Compound preparation and experimental designs. The telaprevir formulations were kindly provided by Vertex Pharmaceuticals. A telaprevir suspension was prepared as described previously (Perni *et al.*, 2006) and used in experiments 1 and 2. In the other experiments, a telaprevir suspension was prepared daily as in the tablet formulation (Forestier *et al.*, 2007; Hézode *et al.*, 2009; McHutchison *et al.*, 2009). A suspension of telaprevir was administered via oral gavage.

Experiment 1: preliminary dose-finding study. Ten out of 11 mice developed serum HCV loads greater than 10^4 copies ml^{-1}. Nine mice with high viral loads (>10^5 copies ml^{-1}) were randomized and administered 10 or 100 mg telaprevir kg^{-1} BID or TID over three periods. During period 1, the mice were administered 100 (n=4) or 10 (n=4) mg telaprevir kg^{-1} or vehicle (n=1) BID at 18:00 and 10:00 h for 7 days, and serum samples were collected before treatment and 1 h after administration in the morning on the third and/or seventh day. During period 2, the mice were administered 100 (n=5) or 10 (n=4) mg telaprevir kg^{-1} TID for 3 days, and serum samples were collected before treatment and 4 h after administration of the last dose. Three mice died between periods 2 and 3. During period 3, the mice were administered 100 (n=3) or 10 (n=3) mg telaprevir kg^{-1} TID for 10 days. The mice were sacrificed 5 h after administration of the last dose, and plasma, serum and liver samples were collected.

Experiment 2: evaluation of HCV turnover. Eleven mice were infected with HCV and eight mice survived for more than 15 weeks with steady-state and high viral loads (10^6–10^8 copies ml^{-1}). Six of the mice were administered 200 mg telaprevir kg^{-1} TID at 9:00, 14:00 and 19:00 h for 4 days. On day 1, serum samples were collected before dose administration, 4 h after the first and second doses were administered, and 2 h after the third dose was administered (n=2 each). On day 2, serum samples were collected 1 h after each of the three doses was administered (n=2 each). Serum samples were also collected 4 h after the first and second doses were administered on day 3 (n=3 each) and 4 h after the second dose was administered on day 4.

Experiment 3: PK analysis. After a washout period, six mice from experiment 2 were administered 100 or 300 mg telaprevir kg^{-1} (n=3 each) BID at 19:00 and 9:00 h for 4 days. Serum samples were collected before dose administration, 4 (n=1) or 8 (n=2) h after administration of the second dose, and 5 h after every two doses were administered. After the final dose was administered, plasma for PK analysis was collected at 1 and 4 h. The mice were sacrificed at 8 h, and serum, plasma and liver samples were collected.

Experiment 4: dose dependence and PK/PD analysis. Thirty-six mice were infected with HCV and 13 survived for more than 13 weeks. The median survival time of this cohort was 81 days after infection. Twelve HCV-infected mice were randomized into three groups (A–C; n=4 each) and underwent two periods of BID dosing for 5 days, which were separated by 1-week washout periods. During the first period, the mice in groups A, B and C were administered 300 mg telaprevir kg^{-1}, 100 mg telaprevir kg^{-1} and vehicle,

respectively. Because two mice in group A and two mice in group C died before the second period, two remaining mice in group C and one back-up mouse were assigned to group A (n=2) and group B (n=1). During the second period, mice that received high or low doses were crossed over to the alternative treatment. Serum samples were collected before the first dose was administered and 5 h after every two doses were administered. Plasma samples were also collected at the same time on days 1, 3 and 5 in the first period and days 1, 3 and 4 in the second period. The mice were sacrificed 8 h after administration of the final dose, and serum, plasma and liver samples were collected.

Experiment 5: viral kinetics with BID dosing After infection of 45 mice, 12 HCV-infected mice maintained steady-state and high viral loads (1.2×10^6–8.5×10^7 copies ml^{-1}) for more than 6 months. The median survival time of this cohort was 131 days after infection. These mice were treated with 200 mg telaprevir kg^{-1} BID at 19:00 and 9:00 h for 3 days. The mice were divided into two groups and serum samples were collected just before the second dose was administered and 4 (n=6) or 8 (n=6) h after every two doses were administered.

Serum RNA extraction and HCV RNA quantification. HCV RNA was isolated from 10 µl serum under denaturing conditions using a SepaGene RV-R kit (Sanko Junyaku). The dried precipitates were dissolved in 10 µl diethylpyrocarbonate-treated water. Extracts were duplicated and assayed by quantitative real-time RT-PCR using TaqMan EZ RT-PCR core reagents (Applied Biosystems). Nucleotide positions of the probe and primer sets refer to HCV H77 strain (GenBank accession no. AF009606). The TaqMan probe 5′-6-FAM-CTGCGGAACCGGTGAGTACAC-BHQ-1-3′ (nt 148–168) was purchased from Biosearch Technologies, and the forward (5′-CGGGAGAGCCATAGTGG-3′; nt 130–146) and reverse (5′-AGTACCACAAGGCCTTTCG-3′; nt 272–290) primers were purchased from Sigma-Aldrich. The 25 µl RT-PCR mixture contained 0.2 nmol forward and reverse primers ml^{-1}, 0.3 nmol TaqMan probe ml^{-1} and 5 µl extracted RNA, and was monitored using a PRISM 7900HT sequence detection system (Applied Biosystems). The thermal profile was 2 min at 50 °C, 30 min at 60 °C for reverse transcription and 5 min at 95 °C, followed by 45 cycles of 20 s at 95 °C and 1 min at 62 °C. The HCV replicon I_{389}neo/NS3-3′/5.1 (Lohmann *et al.*, 1999) RNA was transcribed *in vitro* using a T7 RiboMax Express Large Scale RNA Production System (Promega) and purified twice using gel filtration. The concentration of this transcribed RNA was determined by absorbance at 260 nm and serially diluted 10-fold to prepare a standard curve for each assay.

Liver RNA extraction and HCV RNA quantification. A Wizard SV total RNA Isolation System (Promega) was used to obtain a DNase I-treated total RNA sample. The total RNA concentration was determined by absorbance at 260 nm. Total RNA samples were assayed by duplex real-time RT-PCR for relative quantification of HCV RNA using endogenous control gene expression of human β_2-microglobulin (hβ_2m; GenBank accession no. NM_004048), the TaqMan probe 5′-CAL Fluor Orange 560-AGTGGGATCG-AGACATGTAAGCAGCATCAT-BHQ-1-3′ (nt 401–430), and the forward and reverse primer set of 5′-TTGTCACAGCCCAA-GATAGTT-3′ (nt 379–399) and 5′-TGCGGCATCTTCAAACC-3′ (nt 434–450). To adjust the efficacy of PCR amplification of both target genes, the reaction condition was modified from the HCV single-probe assay. The temperature for extension was 60 °C, the concentration of the HCV probe was 0.24 nmol ml^{-1} and the reaction mixture contained the TaqMan probe/primer set for hβ_2m: 0.2 nmol primers ml^{-1} and 0.12 nmol TaqMan probe ml^{-1}. Because both target genes double after one cycle of PCR, a difference in Ct between HCV and hβ2m ($\Delta Ct = Ct_{HCV} - Ct_{h\beta2m}$) theoretically indicates a relative quantity of HCV RNA per control gene expression of $2^{-\Delta\Delta Ct}$.

Determination of drug concentration. Plasma and liver samples were analysed using chiral liquid chromatography followed by tandem mass spectrometry. After reconstitution, sample extracts were separated by normal-phase chromatography on a 2 × 250 mm Hypersil CPS-1 column (Thermo Hypersil-Keystone) with a mobile phase of heptane:acetone:methanol (82:17:1). Analyte concentrations were determined by turbo ion spray liquid chromatography/tandem mass spectrometry in the positive-ion mode. Analysis was performed at SRL or Mitsubishi Chemical Medience.

Statistical analysis. The HCV RNA level in serum was normalized by logarithmic conversion. Statistical analysis was performed with a mixed linear model using SAS (SAS Institute). Mean differences between two groups were evaluated with Student's t-test. The difference compared with vehicle control at each time point was evaluated by Dunnett's multiple comparisons test. Linear and non-linear regression analyses were performed using GraphPad Prism 5 (GraphPad Software).

Viral dynamics model analysis. The basic mathematical model for the analysis of HCV infection *in vivo*, which is a system of three ordinary differential equations for uninfected cells (T), productively infected cells (I) and free virus (V), has been reviewed elsewhere (Perelson & Ribeiro, 2008). Briefly, one of the three equations ($dV/dt = pI - cV$), where viral particles are produced at rate p per infected cell and cleared at rate c per virion, was solved. During treatment for 2–3 days, if one assumes that the number of I is approximately constant and equal to its pre-treatment value and that the viral level was at its set-point value (V_0), then $pI = cV_0$. Using this relationship in the equation $dV/dt = (1-\varepsilon)pI - cV$, where ε is the effectiveness in blocking virion production, yields $dV/dt = (1-\varepsilon)\,cV_0 - cV$, $V(0) = V_0$ with the solution $V(t) = V_0(1-\varepsilon+\varepsilon e^{-ct})$. Because the log change of viral load at time [$\log \Delta V(t)$] equals $\log V(t)/V_0$, the solved equation [$\log \Delta V(t) = \log(1-\varepsilon+\varepsilon e^{-ct})$] was fitted to the values obtained in this study via non-linear least-squares regression in order to estimate ε and c.

ACKNOWLEDGEMENTS

We thank Drs Ichimaro Yamada, Mitsubishi Tanabe Pharma Corporation, and Ann D Kwong, Gururaj Kalkeri, Susan Almquist, Steven M. Lyons and John Randle, Vertex Pharmaceuticals, for their thoughtful discussions. This work was supported in part by Grants-in-Aid for scientific research and development from the Ministry of Education, Sports, Culture and Technology and the Ministry of Health, Labour and Welfare, Japan.

REFERENCES

Boonstra, A., van der Laan, L. J. W., Vanwolleghem, T., Harry, L. A. & Janssen, H. L. A. (2009). Experimental models for hepatitis C viral infection. *Hepatology* **50**, 1646–1655.

Chang, M., Williams, O., Mittler, J., Quintanilla, A., Carithers, R. L., Jr, Perkins, J., Corey, L. & Gretch, D. R. (2003). Dynamics of hepatitis C virus replication in human liver. *Am J Pathol* **163**, 433–444.

Dahari, H., Feliu, A., Garcia-Retortillo, M., Forns, X. & Neumann, A. U. (2005). Second hepatitis C replication compartment indicated by viral dynamics during liver transplantation. *J Hepatol* **42**, 491–498.

Forestier, N., Reesink, H. W., Weegink, C. J., McNair, L., Kieffer, T. L., Chu, H.-M., Purdy, S., Jansen, P. L. M. & Zeuzem, S. (2007). Antiviral

activity of telaprevir (VX-950) and peginterferon alfa-2a in patients with hepatitis C. *Hepatology* **46**, 640–648.

Fried, M. W., Shiffman, M., Reddy, K. R., Smith, C., Marinos, G., Gonçales, F. L., Jr, Häussinger, D., Diago, M., Carosi, G. & other authors (2002). Peginterferon alfa-2a plus ribavirin for chronic hepatitis C virus infection. *N Engl J Med* **347**, 975–982.

Herrmann, E., Lee, J.-H., Marinos, G., Modi, M. & Zeuzem, S. (2003). Effect of ribavirin on hepatitis C viral kinetics in patients treated with pegylated interferon. *Hepatology* **37**, 1351–1358.

Hézode, C., Forestier, N., Dusheiko, G., Ferenci, P., Pol, S., Goeser, T., Bronowicki, M.,, Bourlière, J.-P., Gharakhanian, S. & other authors (2009). Telaprevir and peginterferon with or without ribavirin for chronic HCV infection. *N Engl J Med* **360**, 1839–1850.

Hiraga, N., Imamura, M., Tsuge, M., Noguchi, C., Takahashi, S., Iwao, E., Fujimoto, Y., Abe, H., Maekawa, T. & other authors (2007). Infection of human hepatocyte chimeric mouse with genetically engineered hepatitis C virus and its susceptibility to interferon. *FEBS Lett* **581**, 1983–1987.

Katoh, M., Sawada, T., Soeno, Y., Nakajima, M., Tateno, C., Yoshizato, K. & Yokoi, T. (2007). *In vivo* drug metabolism model for human cytochrome P450 enzyme using chimeric mice with humanized liver. *J Pharm Sci* **96**, 428–437.

Katoh, M., Tateno, C., Yoshizato, K. & Yokoi, T. (2008). Chimeric mice with humanized liver. *Toxicology* **246**, 9–17.

Kimura, T., Imamura, M., Hiraga, N., Hatakeyama, T., Miki, D., Noguchi, C., Mori, N., Tsuge, M., Takahashi, S. & other authors (2008). Establishment of an infectious genotype 1b hepatitis C virus clone in human hepatocyte chimeric mice. *J Gen Virol* **89**, 2108–2113.

Kneteman, N. M., Weiner, A. J., O'Connell, J., Collett, M., Gao, T., Aukerman, L., Kovelsky, R., Ni, Z.-J., Hashash, A. & other authors (2006). Anti-HCV therapies in chimeric *scid*-Alb/uPA mice parallel outcomes in human clinical application. *Hepatology* **43**, 1346–1353.

Kneteman, N. M., Howe, A. Y. M., Gao, T., Lewis, J., Pevear, D., Lund, G., Douglas, D., Mercer, D. F., Tyrrell, D. L. J. & other authors (2009). HCV796: a selective nonstructural protein 5B polymerase inhibitor with potent anti-hepatitis C virus activity *in vitro*, in mice with chimeric human livers, and in humans infected with hepatitis C virus. *Hepatology* **49**, 745–752.

Lauer, G. M. & Walker, B. D. (2001). Hepatitis C virus infection. *N Engl J Med* **345**, 41–52.

Liang, T. J., Rehermann, B., Seeff, L. B. & Hoofnagle, J. H. (2000). Pathogenesis, natural history, treatment and prevention of hepatitis C. *Ann Intern Med* **132**, 296–305.

Lindenbach, B. D., Meuleman, P., Ploss, A., Vanwolleghem, T., Syder, A. J., McKeating, J. A., Lanford, R. E., Feinstone, S. M., Major, M. E. & other authors (2006). Cell culture-grown hepatitis C virus is infectious *in vivo* and can be recultured *in vitro*. *Proc Natl Acad Sci U S A* **103**, 3805–3809.

Lohmann, V., Körner, F., Koch, J., Herian, U., Theilmann, L. & Bartenschlager, R. (1999). Replication of subgenomic hepatitis C virus RNAs in a hepatoma cell line. *Science* **285**, 110–113.

Manns, M. P., McHutchison, J. G., Gordon, S. C., Rustgi, V. K., Shiffman, M., Reindollar, R., Goodman, Z. D., Koury, K., Ling, M.-H. & other authors (2001). Peginterferon alfa-2b plus ribavirin compared with interferon alfa-2b plus ribavirin for initial treatment of chronic hepatitis C: a randomised trial. *Lancet* **358**, 958–965.

Manns, M. P., Foster, G. R., Rockstroh, J. K., Zeuzem, S., Zoulim, F. & Houghton, M. (2007). The way forward in HCV treatment – finding the right path. *Nat Rev Drug Discov* **6**, 991–1000.

McHutchison, J. G., Everson, G. T., Gordon, S. C., Jacobson, I. M., Sulkowski, M., Kauffman, R., McNair, L., Alam, J., Muir, A. J. & other authors (2009). Telaprevir with peginterferon and ribavirin for chronic HCV genotype 1 infection. *N Engl J Med* **360**, 1827–1838.

Mercer, D. F., Schiller, D. E., Elliott, J. F., Douglas, D. N., Hao, C., Rinfret, A., Addison, W. R., Fischer, K. P., Churchill, T. A. & other authors (2001). Hepatitis C virus replication in mice with chimeric human livers. *Nat Med* **7**, 927–933.

Neumann, A. U., Lam, N. P., Dahari, H., Gretch, D. R., Wiley, T. E., Layden, T. J. & Perelson, A. S. (1998). Hepatitis C viral dynamics *in vivo* and the antiviral efficacy of interferon-α therapy. *Science* **282**, 103–107.

Pawlotsky, J.-M., Dahari, H., Neumann, A. U., Hezode, C., Germanidis, G., Lonjon, I., Castera, L. & Dhumeaux, D. (2004). Antiviral action of ribavirin in chronic hepatitis C. *Gastroenterology* **126**, 703–714.

Pereira, A. A. & Jacobson, I. M. (2009). New and experimental therapies for HCV. *Nat Rev Gastroenterol Hepatol* **6**, 403–411.

Perelson, A. S. & Ribeiro, R. M. (2008). Estimating drug efficacy and viral dynamic parameters: HIV and HCV. *Stat Med* **27**, 4647–4657.

Perni, R. B., Almquist, S. J., Byrn, R. A., Chandorkar, G., Chaturvedi, P. R., Courtney, L. F., Decker, C. J., Dinehart, K., Gates, C. A. & other authors (2006). Preclinical profile of VX-950, a potent, selective, and orally bioavailable inhibitor of hepatitis C virus NS3-4A serine protease. *Antimicrob Agents Chemother* **50**, 899–909.

Powers, K. A., Ribeiro, R. M., Patel, K., Pianko, S., Nyberg, L., Pockros, P., Conrad, A. J., McHutchison, J. & Perelson, A. S. (2006). Kinetics of hepatitis C virus reinfection after liver transplantation. *Liver Transpl* **12**, 207–216.

Poynard, T., Yuen, M.-F., Ratziu, V. & Lai, C. L. (2003). Viral hepatitis C. *Lancet* **362**, 2095–2100.

Quinkert, D., Bartenschlager, R. & Lohmann, V. (2005). Quantitative analysis of the hepatitis C virus replication complex. *J Virol* **79**, 13594–13605.

Ramratnam, B., Bonhoeffer, S., Binley, J., Hurley, A., Zhang, L., Mittler, J. E., Minarkowitz, M., Moore, J. P., Perelson, A. S. & Ho, D. D. (1999). Rapid production and clearance of HIV-1 and hepatitis C virus assessed by large volume plasma apheresis. *Lancet* **354**, 1782–1785.

Reesink, H. W., Zeuzem, S., Weegink, C. J., Forestier, N., Vliet, A., van de Wetering de Rooij,, J., McNair, L, Purdy, S., Kauffman, R. & other authors (2006). Rapid decline of viral RNA in hepatitis C patients treated with VX-950: a phase Ib, placebo-controlled, randomized study. *Gastroenterology* **131**, 997–1002.

Sarrazin, C., Kieffer, T. L., Bartels, D., Hanzelka, B., Möh, U., Welker, M., Wincheringer, D., Zhou, Y., Chu, H.-M. & other authors (2007). Dynamic hepatitis C virus genotypic and phenotypic changes in patients treated with the protease inhibitor telaprevir. *Gastroenterology* **132**, 1767–1777.

Schiano, T. D., Gutierrez, J. A., Walewski, J. L., Fiel, M. I., Cheng, B., Bodenheimer, H., Jr, Thung, S. N., Chung, R. T., Schwartz, M. E. & other authors (2005). Accelerated hepatitis C virus kinetics but similar survival rates in recipients of liver grafts from living versus deceased donors. *Hepatology* **42**, 1420–1428.

Sherman, K. E., Fleischer, R., Laessig, K., Murray, J., Tauber, W. & Birnkrant, D. (2007). Development of novel agents for the treatment of chronic hepatitis C infection: summary of the FDA antiviral products advisory committee recommendations. *Hepatology* **46**, 2014–2020.

Talal, A. H., Ribeiro, R. M., Powers, K. A., Grace, M., Cullen, C., Hussain, M., Markatou, M. & Perelson, A. S. (2006). Pharmacodynamics of PEG-IFN α differentiate HIV/HCV coinfected sustained virological responders from nonresponders. *Hepatology* **43**, 943–953.

Tateno, C., Yoshizane, Y., Saito, N., Kataoka, M., Utoh, R., Yamasaki, C., Tachibana, A., Soeno, Y., Asahina, K. & other authors (2004). Near completely humanized liver in mice shows human-type metabolic responses to drugs. *Am J Pathol* **165**, 901–912.

Tsuge, M., Hiraga, N., Takaishi, H., Noguchi, C., Oga, H., Imamura, M., Takahashi, S., Iwao, E., Fujimoto, Y. & other authors (2005). Infection of human hepatocyte chimeric mouse with genetically engineered hepatitis B virus. *Hepatology* **42**, 1046–1054.

Vanwolleghem, T., Meuleman, P., Libbrecht, L., Roskams, T., De Vos, R. & Leroux-Roels, G. (2007). Ultra-rapid cardiotoxicity of the hepatitis C virus protease inhibitor BILN 2061 in the urokinase-type plasminogen activator mouse. *Gastroenterology* **133**, 1144–1155.

Vona, G., Tuveri, R., Delpuech, O., Vallet, A., Canioni, D., Ballardini, G., Trabut, J. B., Le Bail, B., Nalpas, B. & other authors (2004). Intrahepatic hepatitis C virus RNA quantification in microdissected hepatocytes. *J Hepatol* **40**, 682–688.

Wasley, A. & Alter, M. J. (2000). Epidemiology of hepatitis C: geographic differences and temporal trends. *Semin Liver Dis* **20**, 1–16.

Clinical & Experimental Immunology
The Journal of Translational Immunology

Clinical and Experimental Immunology ORIGINAL ARTICLE doi:10.1111/j.1365-2249.2010.04246.x

Prolonged recurrence-free survival following OK432-stimulated dendritic cell transfer into hepatocellular carcinoma during transarterial embolization

Y. Nakamoto,* E. Mizukoshi,* M. Kitahara,* F. Arihara,* Y. Sakai,* K. Kakinoki,* Y. Fujita,* Y. Marukawa,* K. Arai,* T. Yamashita,* N. Mukaida,† K. Matsushima,‡ O. Matsui§ and S. Kaneko*

**Disease Control and Homeostasis, Graduate School of Medicine, †Division of Molecular Bioregulation, Cancer Research Institute, Kanazawa University, §Department of Radiology, Graduate School of Medicine, Kanazawa University, Kanazawa, and ‡Department of Molecular Preventive Medicine, Graduate School of Medicine, University of Tokyo, Tokyo, Japan*

Accepted for publication 19 July 2010
Correspondences: S. Kaneko, Disease Control and Homeostasis, Graduate School of Medical Science, Kanazawa University, 13-1 Takara-machi, Kanazawa 920-8641, Japan.
E-mail: skaneko@m-kanazawa.jp

Summary

Despite curative locoregional treatments for hepatocellular carcinoma (HCC), tumour recurrence rates remain high. The current study was designed to assess the safety and bioactivity of infusion of dendritic cells (DCs) stimulated with OK432, a streptococcus-derived anti-cancer immunotherapeutic agent, into tumour tissues following transcatheter hepatic arterial embolization (TAE) treatment in patients with HCC. DCs were derived from peripheral blood monocytes of patients with hepatitis C virus-related cirrhosis and HCC in the presence of interleukin (IL)-4 and granulocyte-macrophage colony-stimulating factor and stimulated with 0·1 KE/ml OK432 for 2 days. Thirteen patients were administered with 5×10^6 of DCs through arterial catheter during the procedures of TAE treatment on day 7. The immunomodulatory effects and clinical responses were evaluated in comparison with a group of 22 historical controls treated with TAE but without DC transfer. OK432 stimulation of immature DCs promoted their maturation towards cells with activated phenotypes, high expression of a homing receptor, fairly well-preserved phagocytic capacity, greatly enhanced cytokine production and effective tumoricidal activity. Administration of OK432-stimulated DCs to patients was found to be feasible and safe. Kaplan–Meier analysis revealed prolonged recurrence-free survival of patients treated in this manner compared with the historical controls ($P = 0{\cdot}046$, log-rank test). The bioactivity of the transferred DCs was reflected in higher serum concentrations of the cytokines IL-9, IL-15 and tumour necrosis factor-α and the chemokines CCL4 and CCL11. Collectively, this study suggests that a DC-based, active immunotherapeutic strategy in combination with locoregional treatments exerts beneficial anti-tumour effects against liver cancer.

Keywords: dendritic cells, hepatocellular carcinoma, immunotherapy, recurrence-free survival, transcatheter hepatic arterial embolization

Introduction

Many locoregional therapeutic approaches including surgical resection, radiofrequency ablation (RFA) and transcatheter hepatic arterial embolization (TAE) have been taken in the search for curative treatments of hepatocellular carcinoma (HCC). Despite these efforts, tumour recurrence rates remain high [1,2], probably because active hepatitis and cirrhosis in the surrounding non-tumour liver tissues causes *de novo* development of HCC [3,4]. One strategy to reduce tumour recurrence is to enhance anti-tumour immune responses that may induce sufficient inhibitory effects to prevent tumour cell growth and survival [5,6]. Dendritic cells (DCs) are the most potent type of antigen-presenting cells in the human body, and are involved in the regulation of both innate and adaptive immune responses [7]. DC-based immunotherapies are believed to contribute to the eradication of residual and recurrent tumour cells.

To enhance tumour antigen presentation to T lymphocytes, DCs have been transferred with major histocompatibility complex (MHC) class I and class II genes [8] and co-stimulatory molecules, e.g. CD40, CD80 and CD86 [9,10], and loaded with tumour-associated antigens, including tumour lysates, peptides and RNA transfection [11]. To induce natural killer (NK) and natural killer T (NK T) cell activation, DCs have been stimulated and modified to

Table 1. Patient characteristics.

Patient no.	Gender	Age (years)	HLA	TNM stages	No. of tumours	Largest tumour (mm)	Child–Pugh	KPS	Post-TAE Rx
1	M	60	A11 A33	III	5	35	B	100	RFA
2	M	57	A11 A24	III	1	21	B	100	RFA
3	M	57	A11 A31	III	2	39	B	100	RFA
4	M	77	A2 A24	III	2	35	A	100	RFA
5	F	83	A11 A24	III	3	29	B	100	RFA
6	F	74	A2 A24	II	1	35	A	100	RFA
7	F	72	A24 A33	III	3	41	B	100	RFA
8	F	65	A2 A11	II	4	12	B	100	RFA
9	M	71	A2 A11	II	4	16	A	100	RFA
10	M	79	A11 A24	III	2	40	A	100	RFA
11	M	71	A2 A24	II	1	28	A	100	RFA
12	M	56	A2 A26	III	2	25	B	100	RFA
13	M	64	A2 A33	III	2	37	B	100	RFA

M, male; F, female; TNM, tumour–node–metastasis; Child–Pugh, Child–Pugh classification; KPS, Karnofsky performance scores; TAE, transcatheter arterial embolization; Rx, treatment; HCC, hepatocellular carcinoma; HLA, human leucocyte antigen; RFA, percutaneous radiofrequency ablation.

produce larger amounts of cytokines, e.g. interleukin (IL)-12, IL-18 and type I interferons (IFNs)[10,12]. Furthermore, DC migration into secondary lymphoid organs could be induced by expression of chemokine genes, e.g. C-C chemokine receptor-7 (CCR7) [13], and by maturation using inflammatory cytokines [14], matrix metalloproteinases and Toll-like receptor (TLR) ligands [15].

DCs stimulated with OK432, a penicillin-inactivated and lyophilized preparation of *Streptococcus pyrogenes*, were suggested recently to produce large amounts of T helper type 1 (Th1) cytokines, including IL-12 and IFN-γ and enhance cytotoxic T lymphocyte activity compared to a standard mixture of cytokines [tumour necrosis factor-α (TNF-α), IL-1β, IL-6 and prostaglandin E_2 (PGE_2)] [16]. Furthermore, because OK432 modulates DC maturation through TLR-4 and the β_2 integrin system [16,17] and TLR-4-stimulated DCs can abrogate the activity of regulatory T cells [18], OK432-stimulated DCs may contribute to the induction of anti-tumour immune responses partly by reducing the activity of suppressor cells. Recently, in addition to the orchestration of immune responses, OK432-activated DCs have themselves been shown to mediate strong, specific cytotoxicity towards tumour cells via CD40/CD40 ligand interactions [19].

We have reported recently that combination therapy using TAE together with immature DC infusion is safe for patients with cirrhosis and HCC [20]. DCs were infused precisely into tumour tissues and contributed to the recruitment and activation of immune cells *in situ*. However, this approach by itself yielded limited anti-tumour effects due probably to insufficient stimulation of immature DCs (the preparation of which seems closely related to therapeutic outcome [21,22]). The current study was designed to assess the safety and bioactivity of OK432-stimulated DC infusion into tumour tissues following TAE treatment in patients with cirrhosis and HCC. In addition to documenting the safety of this approach, we found that patients treated with OK432-stimulated DCs displayed unique cytokine and chemokine profiles and, most importantly, experienced prolonged recurrence-free survival.

Patients and methods

Patients

Inclusion criteria were a radiological diagnosis of primary HCC by computed tomography (CT) angiography, hepatitis C virus (HCV)-related HCC, a Karnofsky score of $\geq$ 70%, an age of $\geq$ 20 years, informed consent and the following normal baseline haematological parameters (within 1 week before DC administration): haemoglobin $\geq$ 8·5 g/dl; white cell count $\geq$ 2000/μl; platelet count $\geq$ 50 000/μl; creatinine $<$ 1·5 mg/dl and liver damage A or B [23].

Exclusion criteria included severe cardiac, renal, pulmonary, haematological or other systemic disease associated with a discontinuation risk; human immunodeficiency virus (HIV) infection; prior history of other malignancies; history of surgery, chemotherapy or radiation therapy within 4 weeks; immunological disorders including splenectomy and radiation to the spleen; corticosteroid or anti-histamine therapy; current lactation; pregnancy; history of organ transplantation; or difficulty in follow-up.

Thirteen patients (four women and nine men) presenting at Kanazawa University Hospital between March 2004 and June 2006 were enrolled into the study, with an age range from 56 to 83 years (Table 1). Patients with verified radiological diagnoses of HCC stage II or more were eligible and enrolled in this study. In addition, a group of 22 historical controls (nine women and 13 men) treated with TAE without DC administration between July 2000 and September 2007 was included in this study. All patients received RFA therapy to increase the locoregional effects 1 week later [24].

They underwent ultrasound, computed tomography (CT) scan or magnetic resonance imaging (MRI) of the abdomen about 1 month after treatment and at a minimum of once every 3 months thereafter, and tumour recurrences were followed for up to 360 days. The Institutional Review Board reviewed and approved the study protocol. This study complied with ethical standards outlined in the Declaration of Helsinki. Adverse events were monitored for 1 month after the DC infusion in terms of fever, vomiting, abdominal pain, encephalopathy, myalgia, ascites, gastrointestinal disorder, bleeding, hepatic abscess and autoimmune diseases.

Preparation and injection of autologous DCs

DCs were generated from blood monocyte precursors, as reported previously [25]. Briefly, peripheral blood mononuclear cells (PBMCs) were isolated by centrifugation in Lymphoprep™ Tubes (Nycomed, Roskilde, Denmark). For generating DCs, PBMCs were plated in six-well tissue culture dishes (Costar, Cambridge, MA, USA) at $1{\cdot}4 \times 10^7$ cells in 2 ml per well and allowed to adhere to plastic for 2 h. Adherent cells were cultured in serum-free media (GMP CellGro® DC Medium; CellGro, Manassas, VA, USA) with 50 ng/ml recombinant human IL-4 (GMP grade; CellGro®) and 100 ng/ml recombinant human granulocyte–macrophage colony-stimulating factor (GM-CSF) (GMP grade; CellGro®) for 5 days to generate immature DC, and matured for a further 2 days in 0·1 KE/ml OK432 (Chugai Pharmaceuticals, Tokyo, Japan) to generate OK-DC. On day 7, the cells were harvested for injection, 5×10^6 cells were suspended in 5 ml normal saline containing 1% autologous plasma, mixed with absorbable gelatin sponge (Gelfoam; Pharmacia & Upjohn, Peapack, NJ, USA) and infused through an arterial catheter following Lipiodol (iodized oil) (Lipiodol Ultrafluide, Laboratoire Guerbet, Aulnay-Sous-Bois, France) injection during selective TAE therapy. Release criteria for DCs were viability > 80%, purity > 30%, negative Gram stain and endotoxin polymerase chain reaction (PCR) and negative in process cultures from samples sent 48 h before release. All products met all release criteria, and the DCs had a typical phenotype of $CD14^-$ and human leucocyte antigen (HLA)-DR^+.

Flow cytometry analysis

The DC preparation was assessed by staining with the following monoclonal antibodies for 30 min on ice: anti-lineage cocktail 1 (lin-1; CD3, CD14, CD16, CD19, CD20 and CD56)-fluorescein isothiocyanate (FITC), anti-HLA-DR-peridinin chlorophyll protein (PerCP) (L243), anti-CCR7-phycoerythrin (PE) (3D12) (BD PharMingen, San Diego, CA, USA), anti-CD80-PE (MAB104), anti-CD83-PE (HB15a) and anti-CD86-PE (HA5.2B7) (Beckman Coulter, Fullerton, CA, USA). Cells were analysed on a fluorescence activated cell sorter (FACS0Calibur™ flow cytometer. Data analysis was performed with CELLQuest™ software (Becton Dickinson, San Jose, CA, USA).

DC phagocytosis

Immature DCs and OK432-stimulated DCs were incubated with 1 mg/ml FITC dextran (Sigma-Aldrich, St Louis, MO, USA) for 30 min at 37°C and the cells were washed three times in FACS buffer before cell acquisition using a FACS-Calibur™ cytometer. Control DCs (not incubated with FITC dextran) were acquired at the same time to allow background levels of fluorescence to be determined.

Enzyme-linked immunosorbent assay (ELISA)

DCs were seeded at 200 000 cells/ml, and supernatant collected after 48 h. IL-12p40 and IFN-γ were detected using matched paired antibodies (BD Pharmingen) following standard protocols.

Cytotoxicity assays

The ability of DCs to exert cytotoxicity was assessed in a standard ^{51}Cr release assay [19]. We used the HCC cell lines Hep3B and PLC/PRF/5 [American Type Culture Collection (ATCC), Manassas, VA, USA] and a lymphoblastoid cell line T2 that expresses HLA-A*0201 (ATCC) as target cells. Target cells were labelled with ^{51}Cr. In a 96-well plate, $2{\cdot}5 \times 10^3$ target cells per well were incubated with DCs for 8 h at different effector/target (E/T) ratios in triplicate. Percentage of specific lysis was calculated as follows: (experimental release – spontaneous release)/(maximum release – spontaneous release) × 100. Spontaneous release was always < 20% of the total.

NK cell activity

NK cell cytotoxicity against K562 erythroleukemia target cells was measured by using ^{51}Cr-release assay, according to previously published methods [26], with PBMCs obtained from the patients. All experiments were performed in triplicate. Percentage of cytotoxicity was calculated as follows: {[experimental counts per minute (cpm) – spontaneous cpm]/[total cpm – spontaneous cpm]} × 100.

Intracellular cytokine expression

Freshly isolated PBMCs were stimulated with 25 ng/ml phorbol 12-myristate 13-acetate (PMA; Sigma-Aldrich) and 1 μg/ml ionomycin (Sigma-Aldrich) at 37°C in humidified 7% CO_2 for 4 h. To block cytokine secretion, brefeldin A (Sigma) [27] was added to a final concentration of 10 μg/ml. After addition of stimuli, the surface staining was performed with anti-CD4-PC5 (13B8·2), anti-CD8-PerCP (SK1) and anti-CD56-PC5 (N901) (Beckman

Coulter). Subsequently, the cells were permeabilized, stained for intracellular IFN-γ and IL-4 using the FastImmune™ system (BD Pharmingen), resuspended in phosphate-buffered saline (PBS) containing 1% paraformaldehyde (PFA), and analysed on a flow cytometer (≈ 10 000 gated events acquired per sample).

IFN-γ enzyme-linked immunospot (ELISPOT) assay

ELISPOT assays were performed as described previously with the following modifications [28–30]. HLA-A24 restricted peptide epitopes, squamous cell carcinoma antigen recognized by T cells 2 $(SART2)_{899}$ (SYTRLFLIL), $SART3_{109}$ (VYDYNCHVDL), multi-drug resistance protein 3 $(MRP3)_{765}$ (VYSDADIFL), $MRP3_{503}$ (LYAWEPSFL), $MRP3_{692}$ (AYVPQQAWI), alpha-fetoprotein $(AFP)_{403}$ (KYIQESQAL), AFP_{434} (AYTKKAPQL), AFP_{357} (EYSRRHPQL), human telomerase reverse transcriptase $(hTERT)_{167}$ (AYQVCGPPL) (unpublished), $hTERT_{461}$ (VYGFVRACL) and $hTERT_{324}$ (VYAETKHFL) were used in this study. Negative controls consisted of an HIV envelope-derived peptide ($HIVenv_{584}$). Positive controls consisted of 10 ng/ml PMA (Sigma) or a CMV pp65-derived peptide ($CMVpp65_{328}$). The coloured spots were counted with a KS ELISPOT Reader (Zeiss, Tokyo, Japan). The number of specific spots was determined by subtracting the number of spots in the absence of antigen from the number of spots in its presence. Responses were considered positive if more than 10 specific spots were detected and if the number of spots in the presence of antigen was at least twofold greater than the number of spots in the absence of antigen.

Cytokine and chemokine profiling

Serum cytokine and chemokine levels were measured using the Bioplex assay (Bio-Rad, Hercules, CA, USA). Briefly, frozen serum samples were thawed at room temperature, diluted 1:4 in sample diluents, and 50 µl aliquots of diluted sample were added in duplicate to the wells of a 96-well microtitre plate containing the coated beads for a validated panel of 27 human cytokines and chemokines (cytokine 27-plex antibody bead kit) according to the manufacturer's instructions. These included IL-1β, IL-1Ra, IL-2, IL-4, IL-5, IL-6, IL-7, IL-8, IL-9, IL-10, IL-12p70, IL-13, IL-15, IL-17, basic fibroblast growth factor (FGF), eotaxin, G-CSF, GM-CSF, IFN-γ, interferon gamma-induced protein (IP)-10, monocyte chemoattractant protein (MCP)-1, MIP-1α, MIP-1β, platelet-derived growth factor (PDGF)-BB, regulated upon activation normal T cell-expressed and secreted (RANTES), TNF-α and vascular endothelial growth factor (VEGF). Eight standards (ranging from 2 to 32 000 pg/ml) were used to generate calibration curves for each cytokine. Data acquisition and analysis were performed using Bio-Plex Manager software version 4.1.1.

Arginase activity

Serum samples were tested for arginase activity by conversion of L-arginine to L-ornithine [31] using a kit supplied by the manufacturer (BioAssay Systems, Hayward, CA, USA). Briefly, sera were treated with a membrane filter (Millipore, Billerica, MA, USA) to remove urea, combined with the sample buffer in wells of a 96-well plate, and incubated at 37°C for 2 h. Subsequently, the urea reagent was added to stop the arginase reaction. The colour produced was read at 520 nm using a microtitre plate reader.

Statistical analysis

Results are expressed as means ± standard deviation (s.d.). Differences between groups were analysed for statistical significance by the Mann–Whitney *U*-test. Qualitative variables were compared by means of Fisher's exact test. The estimated probability of tumour recurrence-free survival was determined using the Kaplan–Meier method. The Mantel–Cox log-rank test was used to compare curves between groups. Any *P*-values less than 0·05 were considered statistically significant. All statistical tests were two-sided.

Results

Preparation of OK432-stimulated DCs

Adherent cells isolated from PBMCs of patients with cirrhosis and HCC (Table 1) were differentiated into DCs in the presence of IL-4 and GM-CSF. The cells were stimulated with 0·1 KE/ml OK432 for 3 days; 54·6 ± 9·5% (mean ± s.d.; $n = 13$) of OK432-stimulated cells showed high levels of MHC class II (HLA-DR) and the absence of lineage markers including CD3, CD14, CD16, CD19, CD20 and CD56, in which 30·9 ± 14·2% were CD11c-positive (myeloid DC subset) and 14·8 ± 11·2 were CD123-positive (plasmacytoid DC subset), consistent with our previous observations [20]. As reported [32,33], greater proportions of the cells developed high levels of expression of the co-stimulatory molecules B7-1 (CD80) and B7-2 (CD86) and an activation marker (CD83) compared to DCs prepared without OK432 stimulation (Fig. 1a). Furthermore, the chemokine receptor CCR7 which leads to homing to lymph nodes [13,34] was also induced following OK432 stimulation.

To evaluate the endocytic and phagocytic ability of the OK432-stimulated cells, uptake of FITC-dextran was quantitated by flow cytometry (Fig. 1b). The cells showed lower levels of uptake due to maturation compared to DCs prepared without OK432 stimulation, while the OK432-stimulated cells derived from HCC patients preserved a moderate uptake capacity. As expected, the OK432-stimulated cells produced large amounts of cytokines IL-12 and IFN-γ (Fig. 1c). In addition, they displayed high cyto-